UNIVERSITY OF CALIFORNIA SAN DIEGO

# Classification of NREM Heterogeneity with Machine Learning Approach Reveals Distinct Temporal and Functional Pattern of NREM Sleep

A Thesis submitted in partial satisfaction of the requirements for the degree Master of Science

in

Biology

by

Koorosh Askari

Committee in charge:

Professor Satchidananda Panda, Chair
Professor Susan Golden, Co-Chair
Professor William Joiner
Professor Ashley Juavinett

2020

The Thesis of Koorosh Askari is approved, and it is acceptable in quality and form for publication on microfilm and electronically:

_____

_____

_____

Co-chair

_____

Chair

University of California San Diego

2020

DEDICATION

Dedicated to my mom, my first science teacher

TABLE OF CONTENTS

LIST OF FIGURES

LIST OF TABLES

LIST OF ILLUSTRATIONS

ABBREVIA TIONS

EEG – Electroencephalography

EMG – Electromyography

EOG – Electrooculography

IL1 – Interleukin-1 beta

NREM – Non-Rapid Eye Movement

REM – Rapid Eye Movement

SCN – Suprachiasmatic Nucleus

SWS – Slow-wave-sleep

SF1 – Sleep Fragmentation Day 1

TNF – tumor necrosis factor-alpha

ACKNOWLEDGEMENTS

This thesis is coauthored with Dr. Michael Lam and Fred Monroe. The thesis author was the primary author of this paper.

I would like to acknowledge Professor Satchidananda Panda for his support as the chair of my committee. I'd like to thank him for giving me the opportunity to work in his lab and for providing me with all the resources I needed to conduct my independent research. His constant support and advice helped me to have a better vision of the circadian biology field.

I want to thank Professor Susan Golden as the co-chair of my committee. She instilled in me a better understanding on how to conduct fundamental research in the field of circadian biology.

I'd like to acknowledge the work of all members of Panda Lab in making this project a success. I thank them for fostering a supportive environment throughout my time in the lab.

I'm extremely grateful to my parents, Saeid and Mandana who sacrificed so much in the process of our immigration to the U.S. They wanted to ensure that I have a shot at receiving a world class education and scientific training, and in the future, I will fight to make sure this remains a possibility for others underprivileged students from every corner of the world.

ABSTRACT OF THE THESIS

**Classification of NREM Heterogeneity with Machine Learning Approach Reveals Distinct Temporal and Functional Pattern of NREM Sleep**

by

Koorosh Askari

Master of Science in Biology

University of California San Diego, 2020

Professor Satchidananda Panda, Chair
Professor Susan Golden, Co-Chair

Sleep is a phenomenon that impacts substantial hours of people in 24 hours. The gold standard for sleep measurement in humans is polysomnogram (PSG) consisting of electroencephalography (EEG), electromyography (EMG), and electrooculography (EOG). The combination of brainwave activity, muscular activity, and eye movement delineate different stages of sleep in humans. Sleep in small animal models is also possible with EEG/EMG. Classically, sleep is scored by visual examination on the characteristics of the EEG (frequency and amplitude). In mice, sleep is grossly categorized as rapid eye movement (REM) or non-REM (NREM) sleep. REM sleep has unique characteristics for EEG (high frequency, low amplitude,

desynchronized waveforms) and EMG (near absent due to muscle atonia). For NREM sleep, the patterns for EEG are highly heterogeneous, making fine mapping of NREM sleep technically challenging and error-prone among different scorers. NREM sleep is not uniform. The ability to objectively evaluate the subtle stages of NREM sleep allow us to appreciate the function of NREM sleep. My thesis focuses on developing a technique that better characterizes distinct clusters of NREM sleep based on the differential potential of EEG at different frequencies in both normal and disrupted sleep conditions. We proposed that, by mapping NREM sleep to a finer resolution, we will reveal distinct temporal and functional patterns of NREM sleep. We used the machine learning technique, K-mean Clustering, to subcategorized NREM into eight different clusters with distinct EEG patterns. These clusters exhibit temporal specificity at different phases of sleep. Finally, we demonstrated that different NREM clusters are differentially affected by experimental disruption of sleep. Our method elicits the complexity of NREM sleep, enabling us to investigate whether specific sequences of NREM clusters exist in normal and pathological sleep.

# Introduction:

## The importance of Sleep

Sleep is defined as a natural and reversible state of reduced responsiveness to external stimuli and relative inactivity, accompanied by a loss of consciousness (Rasch, B & Born, J44). Sleep is an essential part of the human daily life cycle which impacts the physical and mental health and overall life's quality. People approximately spend one-third of their lives sleeping. There is an ongoing debate about the explicit function of sleep. However, there is no debate on sleep as a compulsory activity. In a complete sleep deprivation experiment model on rats, all of them died by the end of the third week (Everson et al.19). It takes approximately the same duration for rats to die due to starvation (Everson et al.19). Sleep plays a supportive role in the release of human hormones from the beginning of human birth (Cacciari et al.9). In children and teenagers, a substantial amount of their growth hormone is released during their sleep which has a role in repairing cells and increasing muscle mass (Cacciari et al.9). Sleep also makes an impact on memory consolidation and learning (Rasch, B & Born, J44). During the sleep, recent memories are encoded to be stored in long term memory. It is the time that new pathways are formed in the brain to prepare humans for new information they will receive (Rasch, B & Born, J44). Those benefits are not exclusively for hippocampus related memories; sleep is also important for immunological memories and enhancing the immunological system of the body (Rasch, B & Born, J44). Sleep also plays a role in the clearance of toxic waste from cerebrospinal fluid disease. To illustrate, beta-amyloid is a substance associating with Alzheimer's disease (Cordone et al. 14). It is demonstrated that the level of beta-amyloid is decreasing during sleep. Sleep also has a role in alertness and focusing (Basner et al.3). The psychomotor vigilance test

(PVT) is measuring the reaction time of human response to an eye stimulus (Basner et al.[3]). It is concluded that the reaction rate of humans is significantly decreasing when they do not have enough sleep (Basner et al.[3]).

**Consequences of Lack of Sufficient Sleep**

In the short term, the cognitive and psychological aspects of sleep deprivation are more illustrative. Lack of enough sleep triggers microsleep during the wakefulness (Alhola et al.[1]). These sleep instances will impact on the performance and alertness of a person during an activity (Alhola et al.[1]). It is illustrated in a research that after 40 hours of sleep deprivation in young (18-24 years old) adults, their cognitive performance declined and would resemble elders (63-73 years old) (Alhola et al.[1]). Unfortunately, sometimes it is hard for sleep-deprived people to recognize they cannot function well. To illustrate, many sleep-deprived people do not recognize they are incapable of driving (Williamson et al., 2000). Not only drives but also many workers in other fields have been impacted by sleep deficiency such as medical residents who may make more mistakes and endanger the safety of patients (Kramer[30]).

Lack of enough sleep in the chronic stage impacts numerous physiological factors. Sleep deficiency impaired the repairing mechanism of the heart and vessels, therefore, increasing the risk of cardiovascular disease, high blood pressure, stroke, and cancer increases in sleep-deprived people (Nagai et al.[39]). Sleep has a role in regulating ghrelin and leptin hormones (Taheri et al.[52]). In the absence of sleep, the ghrelin hormone expression increases and leptin hormone expression decreases. As a result, sleep-deprived people feel hungrier and eat more and their weight eventually increases. As people get sleep-deprived, their blood glucose level

increases causing insulin insensitivity. These individuals are more prone to diseases such as Type 2 diabetes mellitus (Mesarwi et al.[37]).

**Sleep Regulation:**

There are two factors that regulate sleep: sleep pressure (Process S) and the circadian clock of the body (Process C) (Borbély et al.[6]). Sleep pressure begins building up due to the production of somnolence on the onset of wakefulness. Somnogens are substances that drive humans into sleep. Examples of somnogens are adenosine, cytokines, Interleukin-1 beta (IL1), and tumor necrosis factor-alpha (TNF) (Krueger[31]). As the level of somnogens increase, they send signals to specific receptors in the brain and send signals to the body to get prepared for sleep. To be more specific, illustration 1 represents adenosine in synaptic region. Adenosine is made from 5′-AMP by different 5′-nucleotidase intracellularly and extracellularly (Lazarus et al.[34]). In case of high level of adenosine, cells take them up and phosphorylate them to AMP by adenosine kinase (Lazarus et al.[34]). Therefore, as the adenosine metabolism increase in the body, more ATP will become dephosphorylated (Lazarus et al.[34]). The dephosphorylation of ATP makes impact on cell metabolism and energy. In Adults' brains, the cells that are responsible for this task are glia cells. Glia cells have equilibrated nucleoside transporters (ENT) which regulates the concentration of adenosine in pre and post synaptic neurons (Lazarus et al.[34]). Under acute sleep deprivation the concentration of adenosine increases in cats measuring with microdialysis (Lazarus et al.[34]). However, during the chronic stage of sleep deprivation the elevated adenosine concentration is no longer observed which means the body is shifted from homeostatic response to allostatic response (Lazarus et al.[34]).

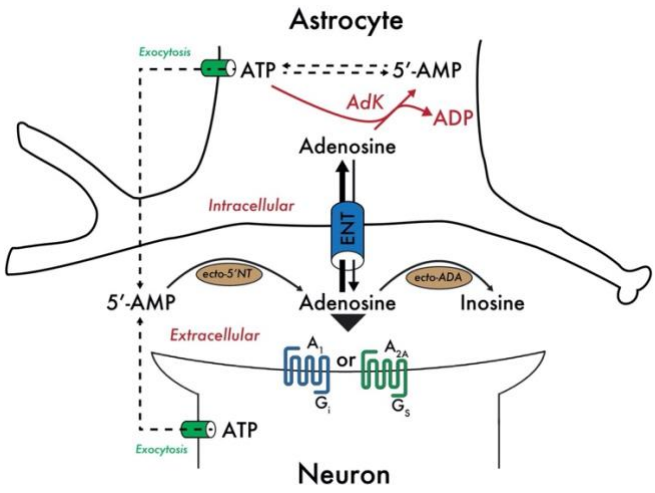


**Illustration 1: Adenosine metabolism impacts the Process S of sleep.**
(Reprint from Lazarus et al.[34])

On the other hand, Process C is regulated by the master clock of the body which is the suprachiasmatic nucleus (SCN). The SCN receives its input from eye receptors called intrinsically photosensitive retinal ganglion cells (ipRGCs). These cells are sending messages through optic nerves to the retinohypothalamic tract (Paul et al.[42]). SCN is regulating different hormonal releasing factors and the temperature of the body. In the presence of light, SCN mediates the hypothalamic-pituitary-adrenal (HPA) axis causing the level of glucocorticoid hormone to increase in the body (Nicolaides et al.[41]). SCN also regulates temperature and as the sun rises, SCN begins raising the temperature of the body to prepare the body for alertness (Hastings et al.[26]). Throughout the day, the level of alertness will be raised. After dusk, the alertness of the body would decrease since SCN is not exposed to the sunlight. Illustration 2 demonstrates the place of SCN in human brain by MRI (Illustration 2A) and summary of SCN impact on the function of body (Illustration 2B).

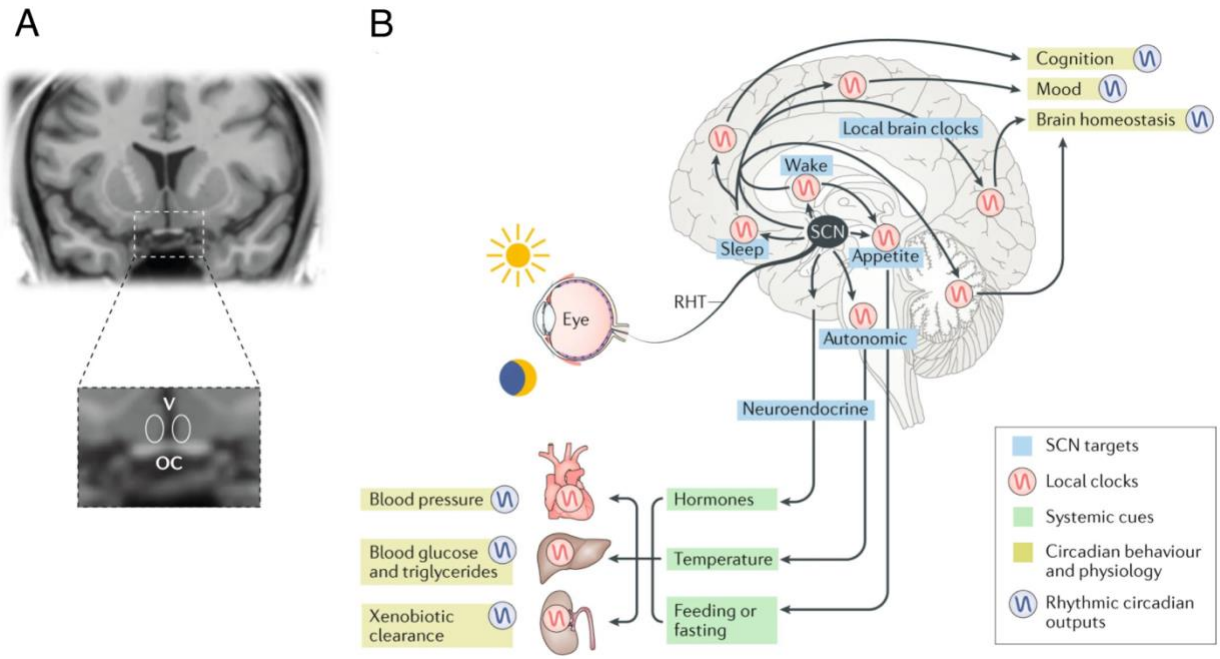


**Illustration 2: The place of SCN in the Brain and its impact on function of body**

(Reprint from Hastings et al.[26])

Together alertness and sleep pressure regulate human sleep. Illustration 3A shows after 16 hours of wakefulness sleep pressure will reach its peak. Meanwhile, Illustration 3B demonstrates around 8 p.m. the alertness of the body will reach its minimum. By looking on both graphs simultaneously, it can be understood that the body is ready for the onset of sleep around 8 p.m. The next morning right before the time that the person wakes up, the sleep pressure is minimal, and the body becomes alert by the light output from the sun and another cycle of the day will begin.

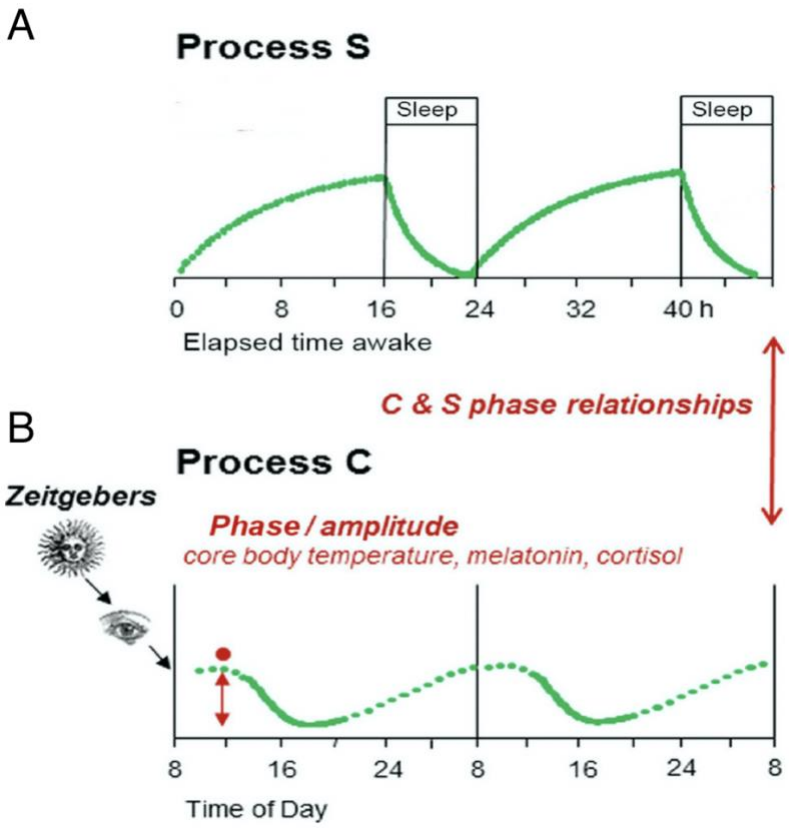


**Illustration 3: The Process C and S temporal pattern**

(Reprint from Borbély et al.[6])

**SCN Mediate Pineal Gland**

SCN is also sending messages to pineal glands and mediates the release of melatonin. Melatonin is commonly named as sleep hormone usually started releasing after the dusk as it appears in Illustration 4A (Borjigin et al.[7]). Melatonin reaches its peak during the night and reach back to a minimal point before the onset of wakefulness. Illustration 4B depicts the pathway that SCN is sending a message to the pineal gland (paraventricular nucleus → intermediolateral →

superior cervical ganglion → pineal gland). This hormone synchronizes external environmental cues with internal biological events (Doghramji[17]).

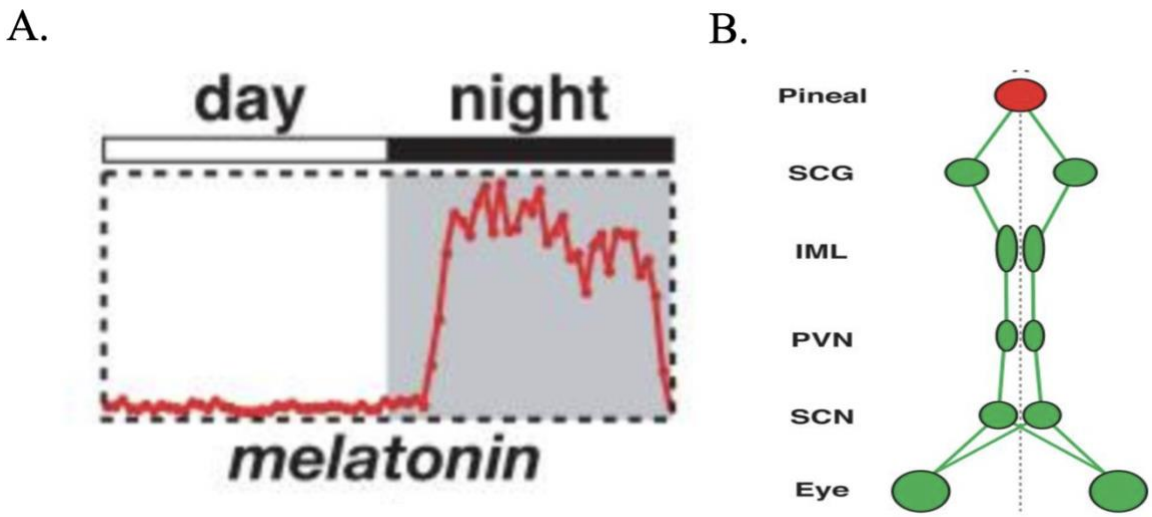


**Illustration 4: SCN impact the release melatonin hormone from pineal gland**

(Reprint from Borjigin et al.[17])

**Disruption of Processes C and S in Modern Society**

The human body clock has evolved through millions of years with respect to the day/night cycle of the earth. As a result, the presence of light in the night disturbed the circadian rhythmicity of the human body. The presence of light with an intensity of 100 lux is enough for half-maximal suppression of melatonin (Gooley et al.[21]). Meanwhile, it is important to notice that a candle that is one meter away from human eyes has an approximate light intensity of 1.0 lux (Bedrosian et al.[4]). Therefore, the light that human body is exposed to at night in shopping centers, houses, or offices is enough to disrupt the rhythmicity of the body. As depicted in illustration 1, this disruption will impact different systems of the body such digestive tract,

urinary system, and circulatory system. In the long term, this disruption in the body rhythmicity can lead to cancer (Haim et al.[23]). Based on illustration 4, the exposure of light makes SCN to send feedback to pineal gland to delay the releasing of melatonin and as a result sleep homeostasis will become disrupted.

Process S can be impacted by beverages such as caffeine which can act as antagonists for adenosine receptor (Lazarus et al., 2019). As a result, the presence of caffeine would decrease the signal sent upon binding of adenosine to its receptor and people may stay awake for longer periods (Lazarus et al.[34]). The half-life of caffeine is ranged differently between humans from 2 to 12 hours (Cappelletti et al.[10]). Therefore, caffeine can shorten the sleep period and negatively impact sleep quality. In case of high dosage of caffeine consumption (600 mg/day), it is illustrated that the blood pressure remains high until 5 days (Cappelletti et al.[10]). As a result, caffeine could also impact the sympathetic nervous system for longer periods causing disruption in homeostasis of the body.

**Sleep Deprivation Ubiquity in the Modern Society:**

Eighty five percent of the U.S. population drinks beverages containing caffeine with an average of 165 mg per day. There are many other social factors that disrupt sleep, such as having a shift working job, frequent traveling, and etc. According to the Centers for Disease Control and Prevention (CDC), 31.6% of adults older than the age of 18 in the U.S experience insufficient sleep. In a study conducted in 2015, 72.7% of high school students and 57.8% of middle school students did not get an adequate amount of sleep. Sleep Apnea is one of the most prevalent sleep disorders and based on the American Academy of Sleep Medicine (Peppard et al.[43]), it is estimated 25 million adults in the U.S. are diagnosed with sleep apnea. Currently, around 6% of

adults are experiencing insomnia. The data mentioned highlights sleep deprivation is an epidemic in the U.S.

**Quantitative Sleep Analysis in Humans:**

Human Sleep is quantitatively evaluated by polysomnography. This is a method that measures sleep based on electroencephalography (EEG), electromyography (EMG), and electrooculography (EOG). According to Illustration 5, there are three pairs of leads placed on the frontal (F3, F4), central (C3, C4), and occipital (01, 02) regions of the brain. There is one pair of EOG leads placed on right and left eyes. EMG leads are placed 1 cm above the inferior edge of the mandible, one two cm below the inferior edge of the mandible and two cm to the right of the midline, and finally another two cm below the inferior edge of the mandible and two cm to the left of the midline. Usually, one EMG channel serves as a backup for making sure at least two channels are recorded.

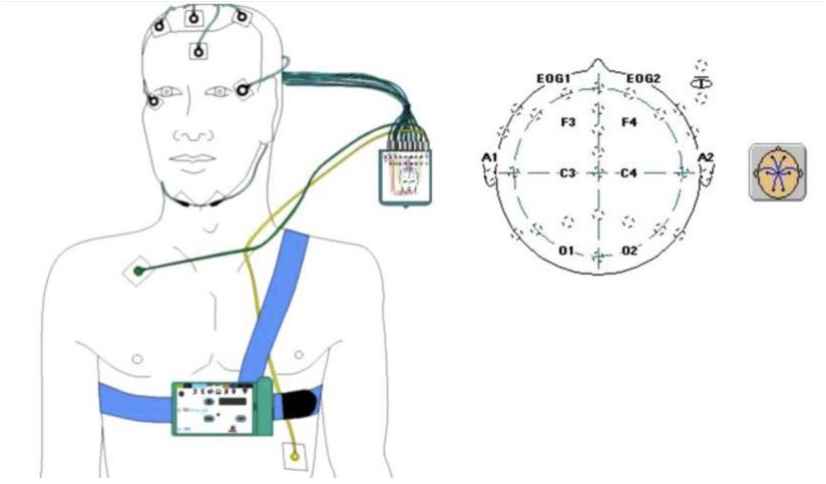


**Illustration 5: Sleep Polysomnography**

(Reprint from Rezaei et al.[45])

Sleep is divided into two main processes Rapid-Eye-Movement (REM) and Non-Rapid Eye-Movement (NREM) sleep. In REM sleep there is a burst of rapid eye movement while in NREM sleep there is no or little eye movement. This phenomenon can be noticed by comparing the EOG signals in illustration 6. REM signal has a higher amplitude as compared to NREM. EMG has the highest activity during wake and lowest activity in Rapid-Eye-Movement (REM) sleep due to skeletal muscle atonia happening in this stage. In addition, the EEG signal has the lowest amplitude and high frequency during REM sleep. On the other hand, during NREM sleep the EEG has the highest amplitude with lower frequency. The EEG during wake time is more synchronized and mixed.

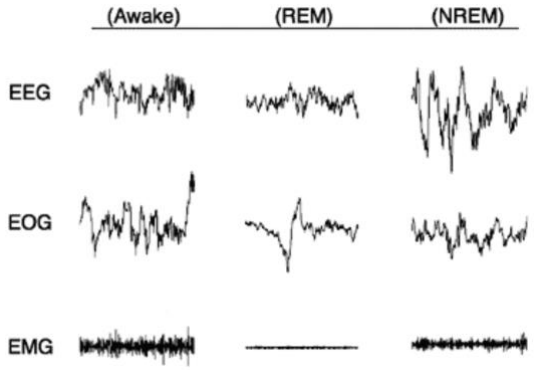


**Illustration 6: Sleep polysomnography data in wake, REM, and NREM**

(Reprint from Lesson 2[35])

NREM sleep itself is subdivided into four stages in humans. Stage 1 which is a transition stage between wakefulness and sleep. As it is illustrated in figure 6, the EEG frequency is still high in stage I of sleep. The second stage of sleep is distinguished from the first stage by the presence of sleep spindles and k-complex. In illustration 7, the k-complex is directed by the arrow and the sleep spindles are underlined. By transitioning from the second stage to the third

stage, the EEG signal amplitude is getting higher and the frequency of the signal decreases. This pattern continues from stage 3 to stage 4. Stages 3 and 4 are also commonly called slow-wave sleep (SWS).

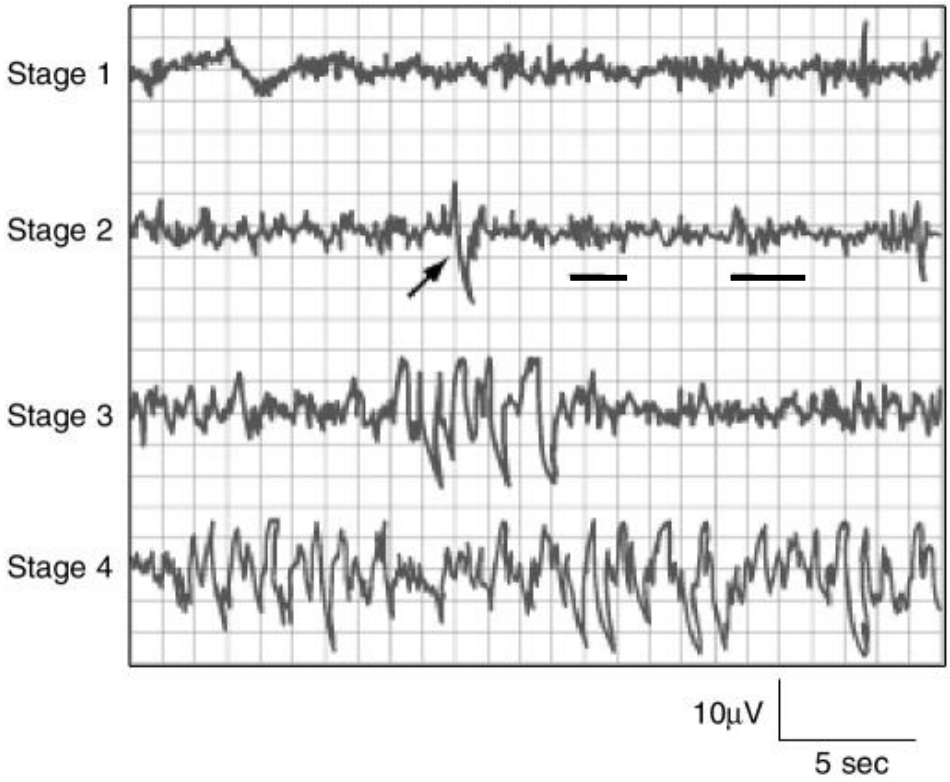


**Illustration 7: NREM Stages of Sleep**

(Reprint from Medicine[36])

**Sleep Cycle in Human:**

Illustration 8 shows sleep architecture in humans. Each cycle of sleep takes approximately 90 minutes and it starts from the first stage of NREM sleep and ends in REM sleep. While there is a distinction in EEG activity during the NREM stages and REM sleep, there is also a difference in time of their occurrence during one night of sleep. As it is demonstrated in

illustration 8, the majority of the SWS happens in the earlier time of the sleep. Toward the end of the sleep, there is almost no time spent in SWS, while REM sleep is occurring more toward the end of the sleep. Each portion of the sleep is responsible for different tasks. For example, memory consolidation for semantic memories is happening in SWS, while the procedural memories are consolidated during REM sleep where most dreaming occurs.

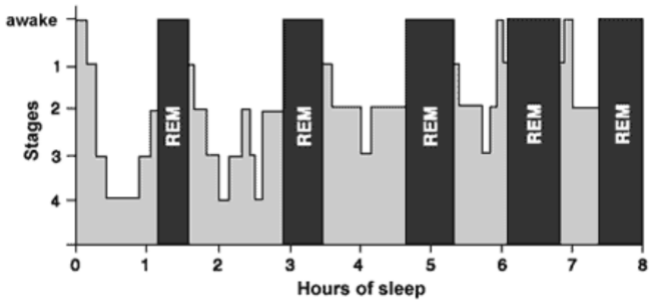


**Illustration 8: Sleep cycles through one night of sleep**

(Reprint from Sleep – Information[50])

**Brainwave involved in Sleep:**

EEG signals are made of distinctive brainwaves frequencies. Illustration 9 represents the frequency corresponding to a particular brainwave and its appearance. For instance, delta waves (0.5 - 4 Hz) have the lowest frequency and higher amplitude, while the gamma waves (>30 Hz) have the highest brainwave frequencies and lower amplitude (Nayak et al.[40]).

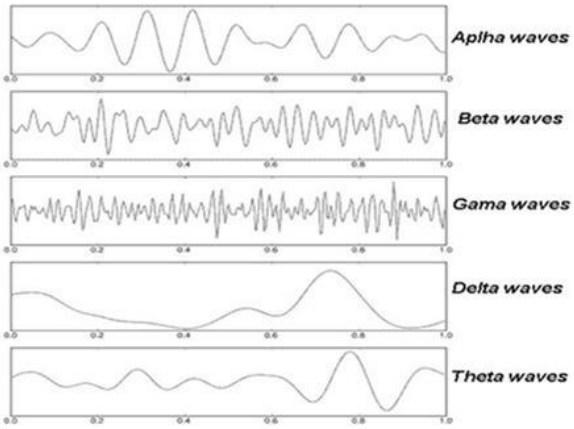


**Illustration 9: Demonstration of Brainwaves in Sleep**

(Reprint Roohi-Azizi et al., 2017)

Each stage of sleep corresponds to a different proportion of these brain wave frequencies. In SWS, the prominent brainwave activity belongs to the delta wave (0.5 to 4 Hz) which notably happens in the frontocentral region of the brain (Nayak et al.[40]). Theta waves occur in the frontocentral region of the brain and move steadily toward the back of the brain during the first and second stages of NREM, these waves are also involved in drowsiness and transitioning to sleep (Nayak et al.[40]). In REM sleep, theta wave is predominant, and the brain activity is more look desynchronized and sawtooth format (Medicine[36]). The Alpha (8-12 Hz) waves are more noticeable in the occipital lobe during wake and REM sleep (Nayak et al.[40]). In addition, alpha wave activity is also high in the prefrontal region during the time of meditation and relaxation. Sigma waves (sleep spindles) are generally present in the frontocentral region of the brain during N2 and their burst lasts for 0.5 to 2 seconds (Nayak et al.[40]). Beta waves are predominant during active attention and focusing. Beta waves also have a role during drowsiness and the N1 stage of sleep (Nayak et al.[40]). These brainwaves begin from the frontocentral region of the head and moves toward the posterior part of the brain and are attenuated as the sleep

moves to the N2 stage. Gamma waves (< 30 Hz) also participate mostly in wakefulness and REM sleep and associate with sensory perception (Nayak et al.[40]). The activity of gamma reaches to the lowest point during SWS (Nayak et al.[40]).

**Advantages and Disadvantages of Using Animal Models in Sleep Studies:**

Using mice to study sleep has extensive advantages. Mice are good models for finding pathways of sleep. They can be genetically mutated in order to find functions of different transmitters involved in sleep (Summa et al.[51]). Also, they can be used for testing new drugs and finding the impact of those substances on sleep (Colavito et al.[13]). On the other hand, there is a limitation in analysis of mice sleeps quantitatively. In mice, it is not possible to record the EOG due to the small size of their skulls. The absence of EOG leads would make the scoring of REM sleep harder in mice. In addition, while there are three pairs of EEG leads that can be used for recording brain activity in humans, there is only one pair of leads that can be implemented in mice. There is no EEG lead on the occipital lobe of mice, so the burst of alpha waves during the REM sleep is not possible to be recognized. In human sleep, NREM sleep is subdivided into four stages; however, conventionally in mice NREM is not subdivided to any substages, and NREM is recognized as one stage in mice. Based on illustration 10, C57BL/6J strain mice spend around 46% of their total time in a day sleeping (Veasey et al.[54]). Approximately this strain of mice spends 92 % of their sleep in NREM (Veasey et al.[54]). Therefore, it is remarkably important to further analyze the NREM sleep to have better understanding of sleep in mice.

| | C57BL/6J (n=10) |
|---|---|
| Time Spent Asleep in 24 Hours (min) | T:665.11±20.7<br>L:449.6±7.9<br>D:215.5±13.8 |
| Percentage of time spent in NREMS | T:42.3%±1.4<br>L:56.9%±1.6<br>D:27.6%±1.8 |
| Percentage of time spent in REMS | T:3.6%±0.5<br>L:5.4%±0.8<br>D:1.8%±0.3 |

**Illustration 10: REM and NREM Percentage in C57BL/6J Mice**

(Reprint Veasey et al.[54])

**Sleep Disruption Model in Mice:**

While there have been multiple attempts to study the normal sleep in mice, there are fewer studies on sleep fragmentation in mice (Kaushal et al.[28]). Illustration 11 represents the cage designed for sleep fragmentation studies in mice. The sweeper travels the bottom of cage within 9 second in every 2 minutes (Kaushal et al.[28]). The methodological approach for this model resembles the obstructive sleep apnea which causes patients to wake up 30 times per hour (Kaushal et al.[28]). This model does not require human subjects for disruption of sleep and minimizes the mice activity during the sleep fragmentation procedure (Kaushal et al.[28]).

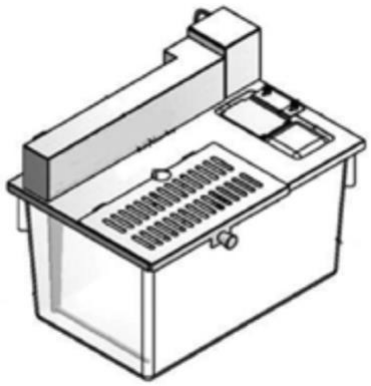

**Illustration 11: Sleep Fragmentation Cage**

(Reprint from Kaushal et al.[28]).

**Impact of Sleep disruption in NREM:**

Illustration 12 shows the result of sleep fragmentation in NREM sleep of C57BL/6J mice. Mice sleep was disrupted only during the light phase (12 hours) based on the model discussed in illustration 11 (Kaushal et al.[29]). As the graph represents, the sleep disruption in the first night causes the NREM sleep time to decrease during the light phase. This reduction is harder to notice after 7 and 15 days of sleep disruption. After the first 12 hours of sleep deprivation, mice experience a rebound during their night phase, but this rebound is less considerable in nights 7 and 15.

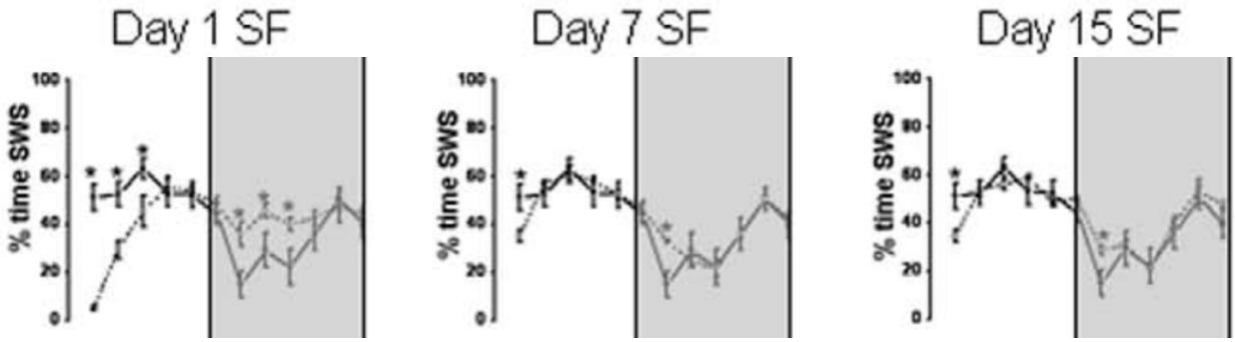


**Illustration 12: Effect of Sleep Fragmentation on NREM Sleep**

The dotted line represents the sleep fragmentation group, and constant line represent the control. (Reprint from Kaushal et al.[29])

**Impact of Sleep Deprivation on Physiology:**

This sleep fragmentation methodology is a powerful model to insert significant biological input on mice bodies. Illustration 13 represents by using same method of fragmentation, tumor cells grow significantly starting on day 21 when comparing sleep fragmented (SF) mice to sleep control (SC) mice (Hakim et al.[24]). During 4 weeks of sleep disruption, the size of the tumor almost doubled in the sleep fragmented group (Hakim et al.[24]).

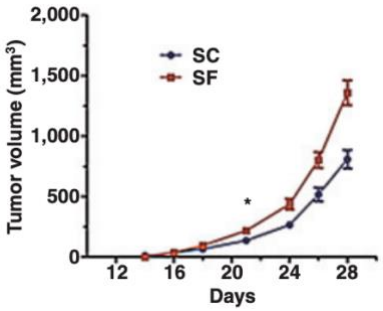


**Illustration 13: Effect of Sleep Fragmentation on Tumor Growth**

(Reprint from Hakim et al.[24])

Moreover, sleep fragmentation increases the risk of obesity as sleep fragmented (SF) mice consume more food in comparison to control (CTL) mice (Wang et al.[55]). Illustration 14 represents the average daily food intake by SF mice is approximately one gram higher in comparison to mice under normal sleep condition. As a result, SF mice weigh significantly more after 4 weeks of sleep fragmentation in comparison to the control group.

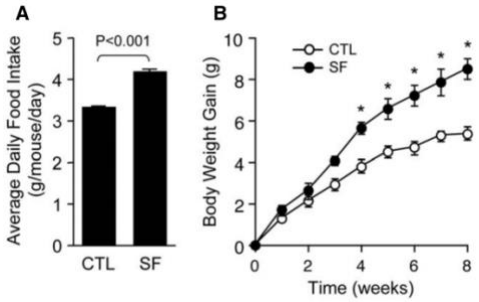


**Illustration 14: Effect of Sleep Fragmentation on Metabolism**

(Reprint from Wang et al.[55])

**Impact of Sleep Disruption on SCN:**

Sleep deprivation impacts rodents' circadian rhythmicity. Illustration 15 A and B represent the light induced phase shift in mice with normal sleep and sleep fragmented mice respectively (Borbély et al.[6]). As is it depicted, the response of animal to light pulse is reduced in

sleep deprivation condition. SCN neuronal activity is also impacted by sleep deprivation (Borbély et al.[6]). Panel C demonstrates the normal SCN activity which is similar to the panel D gray curve. The black curve in panel D represents the SCN activity after sleep deprivation. It can be realized the SCN neuronal activity amplitude decreased during sleep deprivation condition by comparing the black and gray curve in panel D. Illustration 15E represents the firing rate of SCN to a light pulse in normal sleep conditions while panel F represents the firing rate response during sleep deprivation conditions (Borbély et al.[6]). As it is illustrated the SCN firing rate activity in response to light is significantly decreased in rodents when the animal is sleep-deprived (Borbély et al.[6]). As a result, sleep deprivation has an immense impact on SCN and the circadian rhythm of the body in rodents.

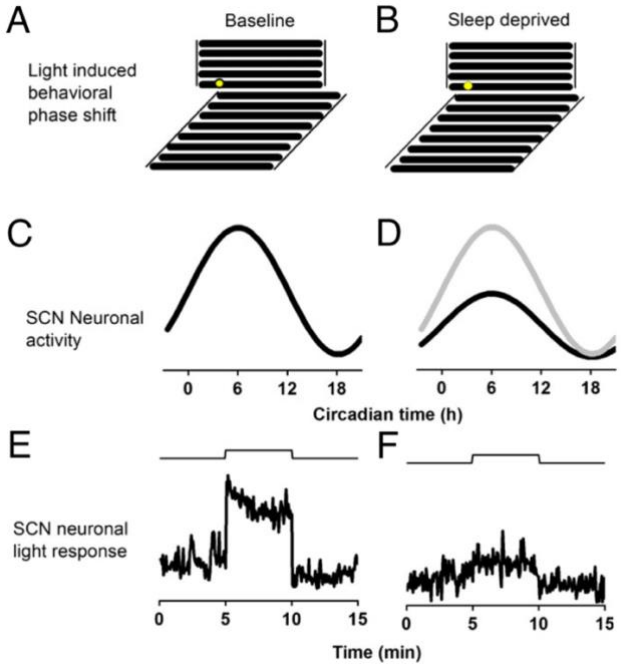


**Illustration 15: Effect of Sleep Deprivation on Circadian Clock of Body**

(Reprint from Borbély et al.[6])

**Hypothesis and K-Mean Clustering**

While it is mentioned in illustration 10, mice spend most of their sleep time in NREM sleep. Like in humans, sleep deprivation in mice can have a significant biological toll on metabolism, tumor growth, and etc. (illustration 13 & 14). However, based on our conventional method of looking at NREM sleep holistically in mice (illustration 12), we could not see the impact of sleep deprivation on NREM sleep. As a result, it is important to find a better method to look at the NREM sleep, so we can better characterize sleep in rodents and quantitate the impact of sleep deprivation in rodents. This paper is introducing a new method for analyzing NREM sleep. We hypothesis that NREM sleep can be further divided into different substages. Each of these substages is unique in terms of their brain wave characteristics and their temporal pattern throughout the light dark cycle of the sleep. We further hypothesize that during the sleep deprivation conditions, the temporal pattern of these NREM substages is impacted distinctively. To investigate our hypotheses, we used a machine learning method called K-Mean Clustering. This is an unsupervised algorithm that subcategorized the data based on the desired number of subcategories (Yuan et al.[59]). The key mathematical algorithm for K-mean clustering is:

$$\mathrm{d} = \sum_{k=1}^{k} \sum_{i=1}^{n} \|(x_i - u_k)\|^2$$

**Illustration 16: K-Mean Clustering Formula**

(Reprint from Yuan et al.[59])

In this formula, k represents the number of clusters and n represents the total number of samples. Based on the given number of clusters (k), this algorithm is looking for a specific centroid ($\mu$) for each cluster (Yuan et al.[59]). The centroids should have a minimal distance from every single data point (x) that is placed on the corresponding cluster (Yuan et al.[59]). According to the formula above the algorithm randomly chooses a different centroid for each cluster and stores the result (Yuan et al.[59]). After running multiple times, it provides the best result for the clustering.

# Method:

### Telemetry Device Implementation and Recording

Three 6 months old C57Bl/6J male mice were used for sleep recording. A telemetric bipotential device (DSI) was surgically implanted in the mouse' abdomen. Two pairs of biopotential leads were directed subcutaneously toward the cervical region. A pair of EEG leads were placed epidurally in left frontal and right parietal lobe, specifically at 1mm anterior and 1mm left lateral to bregma, and 3mm posterior and 3 mm right lateral to bregma. A pair of EMG leads were implanted in the belly muscle of the right Trapezius muscle. The EEG/EMG are recorded continuously for 72 hours per mouse, and the signals were transferred wirelessly to an Acquisition software (DSI). To measure the effects of sleep fragmentation on sleep architecture, mice were housed in a customized chamber equipped with a near-silent motorized sweeping bar. Sleep fragmentation was achieved upon tactile stimulation when the bar sweeps across the bottom of the cage. The bar was set to sweep every 2 minutes during light phase (ZT0 – ZT 12) (Kaushal et al.[28]). Sleep scoring, signal processing and normalization, and k-mean Clustering were performed as indicated above.

### Sleep Scoring

Sleep staging was done manually with visual scoring by Neuroscore software (Fig. 1). The behavioral states of wake, NREM, and REM sleep were assigned for each epoch of 10 second based on EEG, EMG, temperature, and Activity data. A total of 97985 epochs were scored. The number of artifacts, wake, REM and NEM epochs were 777, 51304, 2995, and 42909 respectively.

**K-Mean Clustering**

To fine-map NREM sleep, the electric potentials from 5 frequency bands (Delta, 0.5-4Hz; Theta 4-8Hz; alpha 8-12Hz; Sigma 12-16Hz, and Beta 16 Hz - 24 Hz) were determined by Fourier Transform. The power of each frequency band for each epoch is divided by corresponding total EEG power to find the power ratio for each band. The power ratios were then normalized by the z-score transformation algorithm in python for each brainwave individually (figure 8), and subjected for K-means clustering, with k = 8. The k number is determined based on the silhouette score (figure 9). To validate our method for K-means clustering, we look at the distribution of NREM sleep for three mice in each cluster (table. 3). Table 3 illustrate how each mouse sleep contribute nearly equally to every clusters.

# Result:

### Result of Conventional Sleep Scoring in Mice

In mice, sleep is conventionally scored every ten seconds (an epoch). The software that is used for sleep scoring is named Nueroscore Version 3. The score is made based on the EEG, EMG, activity, and temperature signals. In Fig 1A, there is an example of a wake epoch of a mouse. As it is demonstrated, the EMG amplitude is high, and the activity is above 10 counts/mins. Also, the body temperature was approximately 36 °C. The EEG is desynchronized with a low amplitude and high frequency. Figure 1B represents REM epoch. During REM sleep, the EMG activity signal should be zero as the skeletal muscles in the mouse are in atonia. As it is demonstrated, the EMG signal is in the baseline range, the low EMG signal in this figure represents the pulse rate of the mice. In addition, in REM sleep the EEG signal should have a high frequency and low amplitude. In comparison to the wake epoch (fig 1A), the amplitude of the EEG signal is lower, and the frequency of the EEG signal is also higher. The activity as it is illustrated is zero and the temperature is approximately 35 °C. In similarity to REM sleep, NREM sleep (fig 1C) has a zero-activity signal and the temperature (~ 35.4 °C) is slightly higher than REM sleep. The EMG of NREM sleep is still close to the baseline while it is slightly higher in frequency and amplitude in comparison to REM sleep. However, there is a significant difference in REM and NREM sleep in terms of their EEG pattern. In NREM sleep, the EEG amplitude is higher, and the frequency is lower in comparison to REM sleep.

**Temporal Distribution of NREM and REM Sleep**

Table 1 shows the result of manual sleep scoring data in mice. Based on our scoring, a mouse spends a total of 644 minutes sleeping in 24 hours. The total percentage of time spent in NREM and REM are significantly higher during light phase (ZT 0 -12) in comparing to dark phase (ZT 12 – 24). This is expected as mice are nocturnal animal and spend more time sleeping in presence of light. Our findings are similar to illustration 10 (Veasey et al.[54]). Moreover, Mice in average have 107 seconds sleep bout. Their sleep bout is higher during light phase by 62 seconds in comparison to dark phase (Table. 1). During the fragmented sleep condition, the total time of sleep decreased in mice but not significantly (Table. 1). Mice spent more time sleeping during the dark phase when the bar was not moving (Table. 1). The gap between NREM percentage decreases during acute sleep stress and there were no significant differences between the NREM percentage in light and dark phases in fragmented condition in comparison to normal sleep condition. REM sleep is significantly affected by SF1 condition. The percentage of REM is 0.52% in average for three mice in light phase during SF1, while the percentage for REM sleep in light phase is 5.5 percent during the normal sleep. Meanwhile, the percentage of REM sleep is significantly higher in dark phase in comparison to light phase during the first day of sleep fragmentation (SF1). In average the sleep bout in SF1 was about 77 seconds which was significantly lower in respect to normal sleep condition. Meanwhile, mice had a significant higher sleep bout during the dark phase of SF1. This result was expected as the bar stopped moving during the dark phase.

Figure 2 represents the percentage of recorded time in wake, NREM, and REM during normal and SF1 conditions. While the REM percentage is dramatically suppressed during SF1, there was not a considerable change in NREM sleep during SF1 with respect to normal sleep.

The NREM percentage is significantly lower during the ZT 0 - ZT 2 and ZT 6 – ZT 8 while the NREM percentage increase significantly in ZT 14 – ZT 16 during dark phase of SF1. The wake percentage trend is inversely correlated with NREM percentage for SF1 and normal sleep conditions. On the other hand, REM percentage increase during ZT 14 – ZT 16 and ZT 22 – ZT 24.

Figure 3 demonstrate the distribution of sleep bouts with respect to their percentage in sleep. This figure shows how sleep fragmentation makes significant impact on sleep bout. By looking at light phase during normal sleep condition, it can be perceived mice spend considerable amount of their sleep in bouts with a size larger than 120 seconds. However, there is no sleep bouts presented with a size larger than 110 seconds in SF1 light phase since bar was moving every 2 minutes. As a result, it can be concluded that sleep fragmentation has been done successfully on all three mice.

**K- Mean Clustering Result:**

Figure 5A demonstrates the result of K- Mean clustering based on the relative potential between frequency bands (Delta, Theta, Alpha, Sigma, Beta). Each line of the K-mean clustering result represents one NREM epoch and there are total of 42909 NREM epochs employed in this analysis. Cluster numbers are assigned in order of least delta potential to high delta potential. Cluster 1 has the highest alpha and sigma potentials. In Cluster 2, there is an increase in theta potential while the alpha and sigma potentials are reduced. In Cluster 3, the theta potential reached to the highest level, while the alpha, sigma, and beta potentials are further reduced. While there is a slight change in delta potential from cluster 1 to 3, cluster 4 has a higher level of increase in delta potential. In addition, there is an inverse pattern in theta, alpha, sigma and beta potentials in cluster 4 in respect to cluster 3. In Cluster 5, there is a slight increase in delta

potential. The pattern for alpha, sigma, beta potentials generally resembles cluster 3, while cluster 3 has a higher theta potential than cluster 5. Cluster 6 has a relatively same theta potential as cluster 5 and lower alpha, sigma, and beta potentials. The delta potential is noticeably increased in cluster 6 with respect to clusters 4 and 5. Cluster 7 and 8 have relatively low theta, alpha, sigma, and beta potentials. Cluster 8 has the highest delta potential, and cluster 7 has the second-highest delta potential.

Figure 5b demonstrates the example of EEG and EMG of NREM epochs corresponding to different clusters. In general pattern, the frequency of EEG data is decreasing as the number of clusters is increasing. The amplitude of EEG signal is increasing with respect to cluster number. This result was expected since the cluster associated with higher numbers (7 and 8) can be identified as slow wave sleep in mice due presence of highest delta potentials in them, so the EEG signal for epochs in these two clusters should have a high amplitude and low frequency. However, the clusters associate with lower numbers more so resemble early stage of sleep in humans. As a result, their EEG signal should be more desynchronized with high frequency.

**Temporal Distribution of the Clusters:**

Several NREM clusters have distinct temporal distributions. Figure 6 represents the temporal distribution pattern of each NREM cluster. Each box in fig. 6 represents the 2 hours duration during a 24 hours light dark cycle. The cluster associated with higher delta potentials (6,7, and 8) have early peaks during the light phase. There is only one cluster that has a peak during active phase (dark cycle) which is cluster 3. The rest of NREM substages have peaks closer toward the end of the light phase.

**Impact of Acute Sleep disruption on NREM Clusters:**

Based on Table 2, there is no significant difference between the percentage of clusters 1, 2, and 3 in light and dark phases. However, the rest of clusters percentages are significantly higher during light phase. Cluster 8 has the highest difference in its percentages between light and dark phases. In SF1 condition, there is no significant difference between the percentage of clusters in light and dark phases. Moreover, the total percentage of cluster 1 decrease and the percentage of cluster 3 increase in SF1 in comparison to normal sleep. Clusters 1, 2 and 4 percentages are suppressed significantly during the light phase in SF1 condition. Cluster 4 and 8 percentages are significantly increased during SF1 in comparison to normal sleep during dark phase.

Figure 7 demonstrates the result of night sleep disruption in total NREM sleep and NREM substages. As it is illustrated in figure 7a, the total NREM sleep decreases during sleep disruption but not significant enough (Table 1). This panel does not provide enough information on how NREM sleep epochs with higher delta potentials get impacted by sleep deprivation. By looking at the rest of the panels, it can be understood that acute sleep disruption impacts NREM sleep. In general, the percentage recorded time for clusters with lower delta potentials such as clusters 1, 2, and 4 (figures 6B, C, and E) are reduced by sleep deprivation during dark phase. Cluster 4 has a sharp peak in ZT 20 – 22 during SF1. Although there is not a significant change in clusters 3 and 6 percentages during light phase in normal sleep and SF1 conditions (Table 2), cluster 3 has higher peaks during ZT 10 – ZT 12 and ZT 12 – ZT 14 in SF1 condition. Moreover, cluster 6 has higher peaks during ZT 4 – ZT 6 and ZT 6 – ZT 8. For cluster 5, the cluster percentage decreased during the ZT 0 – ZT 2 during SF1 condition compared to normal sleep, however, the rest of graph points are overlapping between SF1 and normal sleep conditions.

There is no significant change in percentage of cluster 7 in both light and dark phases during SF1 and normal sleep conditions (Table 2). However, the percentage of cluster 7 decreases during ZT 0 – ZT 2 and ZT 4 – ZT 6 in SF1 condition. There is a sharp peak for cluster 7 during ZT 20 – ZT 22 in SF1 condition. Lastly, cluster 8 has a sharp peak during ZT 20 – ZT 22 in SF1 condition and the percentage of cluster 8 during dark phase is significantly higher in the SF1 condition in comparison to normal sleep condition.

# Discussion:

**Impact of Sleep Disruption on NREM Sleep Regulation:**

NREM sleep has a significant higher percentage during light phase, however, the percentage of NREM sleep is not different between dark and light phases during SF1 (Table 1). This result shows how sleep homeostasis is impacted by sleep deprivation. Based on illustration 15, SCN neuronal activity decreases in sleep deprived mice; therefore, process C is impacted by sleep deprivation, so the wake-sleep cycle is impaired in mice.

Moreover, the percentage of NREM sleep increases during wakefulness due to sleep pressure that has been build up in SF1 condition. Sleep pressure is regulated by level of different somnogens such as cytokines (Krueger[32]). interleukin-1 beta (IL1) and tumor necrosis factor alpha (TNF) are two well-known cytokines. (Krueger[32]). Central or systematic injection of either of those cytokines can increase NREM sleep and delta power in mice. Knockout TNF receptor mice do not experience sleep rebound during dark phase after 12 hours of sleep fragmented condition in light phase (Krueger[32]). The mice used in this experiment were wild type and the same strain as in Krueger's experiments (C57Bl/6J). Therefore, it can be concluded that both processes C and S are impacted during SF1. However, it is difficult to pinpoint if the increase in NREM sleep is associated with changes in process C or process S during SF1.

**Impact of Sleep Disruption on REM Sleep Regulation**

While there is a debate on the significance of the impact process C and S have on NREM sleep, there are many experiments revealing REM sleep is regulated by process C more exclusively both in humans (Czeisler et al.[16]) and in mice (Richardson et al., 1985 and Hasan et al., 2018). Figure 2.C represents the recorded percentage of REM sleep during normal sleep and SF1. During the 12 hours of sleep deprivation, the percentage of REM is severely suppressed, and the amount of REM sleep increases significantly during ZT 16 – ZT 18 and ZT 22 – ZT 24 in SF1 in comparison to normal sleep. The absence of REM sleep during the SF1 may be due to the time that is needed after onset of sleep for REM sleep to occur. Figure 4 represent the percentage of REM latency abundance for each REM latency interval during a 24 hours light/dark cycle. Based on table 1, 80% of REM sleep is happening during the light phase in normal sleep. Figure 4A represents that among all the REM epochs through the 24 hours of normal sleep, around 65 % and 12% of REM epochs have REM latency higher than 70 seconds during light and dark phase respectively. Moreover, 14% and 7% of total REM epochs have the REM latency shorter than 70 seconds in light and dark phases respectively (Figure 4A). As a result, the largest portion of REM sleep has REM latency with 70 seconds or higher. In SF1, the total sleep bout during light phase was 69 seconds, therefore, REM sleep was suppressed during SF1 light phase since sleep bout was not long enough for REM sleep occurrence. Therefore, in the future experiments we may need to increase the time interval of Bar movement based on the REM latency result to see how REM sleep temporal pattern will be changed, and confirm the previous experiments on the REM sleep regulation by process C.

**Impact of Sleep disruption on NREM Clusters:**

Our new approach on clustering NREM sleep could explain the impact of sleep deprivation on Processes C and S of NREM with a finer resolution. Cluster 4 and 8 percentages are significantly increased in SF1 condition compared to normal sleep. Our hypothesis is that these clusters may be regulated by process S more exclusively than the other clusters. Moreover, cluster 4 and 8 have significant increases during ZT 20 - ZT 22-time interval in SF1. Cluster 7 also has a same significant increase during the same time interval; however, the percentage of this cluster does not change during dark phase of SF1 in respect to normal sleep. As a result, there is a possibility that cluster 7 is also being regulated by process S. Cluster 1 and 2 have the lowest delta power, as a result, those clusters are more resemblant to REM sleep which also has a low delta power. Like REM sleep the total duration of clusters 1 and 2 are significantly decreased in SF1 in comparison to normal sleep. As a result, these clusters may be regulated by process C more substantially. The temporal pattern of cluster 5 is similar in both SF1 and normal sleep, so this cluster may be regulated robustly by process C. Clusters 3 and 6 are unique because their percentage increase during specific time intervals ZT 10 – ZT 12 and ZT 4 – ZT 8 respectively during SF1 in comparison to normal sleep. Further investigation is needed to address a reason for this increase.

To test these hypotheses, we will set up two different types of experiments in our future direction. First, this experiment can be repeated in DD condition instead of LD condition, to see how the percentage and temporal pattern of these clusters are changing. The clusters that do not have different temporal patterns during the DD cycle are most likely regulated by process C of sleep. Secondly, we can use transgenic TNF receptor knocked-out mice and repeat the experiments. If there are no changes observed in clusters 4,7,8 percentage’s in SF1 dark phase, then those clusters are more likely associated with process S.

**Impact of Sleep Deprivation on Physiology:**

While this paper focused on acute sleep fragmentation, mentioned experiments can be repeated under chronic sleep deprivation conditions. Illustrations 13 and 14, demonstrate that our current sleep fragmentation model can make an impact on tumor growth and metabolism approximately within three weeks of chronic sleep fragmentation. Therefore, we can repeat the experiments and find out which clusters will be suppressed substantially through three weeks of fragmentation. Those clusters of NREM sleep may be related to the physiological outcome of sleep deprivation in mice. Moreover, it has been confirmed that a time restricted feeding diet improves the sleep – wake cycle in mice (Hou et al.[27]). While this diet prevents mice from diagnosis with metabolic diseases (Chaix et al.[11]), with these new NREM clustering techniques we can find out which clusters' percentages in NREM sleep increase under this diet. Consequently, we can have a better insight of how sleep is connected to metabolism.

# Conclusion:

Collectively, we have developed a novel method for characterizing different clusters of NREM sleep revealing both temporal and functional specificity. Our method illustrates that there are total of 8 NREM substages that have distinct brainwave patterns. Some clusters have early peaks during the light phase that are associated with higher delta potentials, and the other clusters usually have higher peaks during the end of the light phase. The impact of acute sleep deprivation on those clusters are distinctive, and not all the clusters are impacted during acute sleep deprivation. This method enables sleep scientists to have a better understanding of sleep and the impact of acute sleep deprivation on mice.

# Citations:


1. Alhola, P. & Polo-Kantola, P. Sleep deprivation: Impact on cognitive performance. *Neuropsychiatr Dis Treat* **3**, 553-567 (2007).

2. Andrillon, T., Nir, Y., Staba, R.J., Ferrarelli, F., Cirelli, C., Tononi, G. & Fried, I. Sleep spindles in humans: insights from intracranial EEG and unit recordings. *J Neurosci* **31**, 17821-17834 (2011).

3. Basner, M. & Dinges, D.F. Maximizing sensitivity of the psychomotor vigilance test (PVT) to sleep loss. *Sleep* **34**, 581-591 (2011).

4. Bedrosian, T.A. & Nelson, R.J. Timing of light exposure affects mood and brain circuits. *Transl Psychiatry* **7**, e1017 (2017).

5. Ben Simon, E., Vallat, R., Barnes, C.M. & Walker, M.P. Sleep Loss and the Socio-Emotional Brain. *Trends Cogn Sci* **24**, 435-450 (2020).

6. Borbely, A.A., Daan, S., Wirz-Justice, A. & Deboer, T. The two-process model of sleep regulation: a reappraisal. *J Sleep Res* **25**, 131-143 (2016).

7. Borjigin, J., Zhang, L.S. & Calinescu, A.A. Circadian regulation of pineal gland rhythmicity. *Mol Cell Endocrinol* **349**, 13-19 (2012).

8. Bringmann, H. Genetic sleep deprivation: using sleep mutants to study sleep functions. *EMBO Rep* **20**(2019).

9. Cacciari, E., Coccagna, G., Cicognani, A., Pirazzoli, P., Gallassi, R., Farneti, P., Bernardi, F., Zappulla, F., Gobbi, G. & Verucchi, P. Growth hormone release during sleep in growth-retarded children with normal response to pharmacological tests. *Arch Dis Child* **53**, 487-490 (1978).

10. Cappelletti, S., Piacentino, D., Sani, G. & Aromatario, M. Caffeine: cognitive and physical performance enhancer or psychoactive drug? *Curr Neuropharmacol* **13**, 71-88 (2015).

11. Chaix, A., Zarrinpar, A., Miu, P. & Panda, S. Time-restricted feeding is a preventative and therapeutic intervention against diverse nutritional challenges. *Cell Metab* **20**, 991-1005 (2014).

12. Chung, S., Lee, E.J., Cha, H.K., Kim, J., Kim, D., Son, G.H. & Kim, K. Cooperative roles of the suprachiasmatic nucleus central clock and the adrenal clock in controlling circadian glucocorticoid rhythm. *Sci Rep* **7**, 46404 (2017).

13. Colavito, V., Fabene, P.F., Grassi-Zucconi, G., Pifferi, F., Lamberty, Y., Bentivoglio, M. & Bertini, G. Experimental sleep deprivation as a tool to test memory deficits in rodents. *Front Syst Neurosci* **7**, 106 (2013).

14. Cordone, S., Annarumma, L., Rossini, P.M. & De Gennaro, L. Sleep and beta-Amyloid Deposition in Alzheimer Disease: Insights on Mechanisms and Possible Innovative Treatments. *Front Pharmacol* **10**, 695 (2019).

15. Czeisler, C.A. & Gooley, J.J. Sleep and circadian rhythms in humans. *Cold Spring Harb Symp Quant Biol* **72**, 579-597 (2007).

16. Czeisler, C.A., Zimmerman, J.C., Ronda, J.M., Moore-Ede, M.C. & Weitzman, E.D. Timing of REM sleep is coupled to the circadian rhythm of body temperature in man. *Sleep* **2**, 329-346 (1980).

17. Doghramji, K. Melatonin and its receptors: a new class of sleep-promoting agents. *J Clin Sleep Med* **3**, S17-23 (2007).

18. Duffy, J.F. & Czeisler, C.A. Effect of Light on Human Circadian Physiology. *Sleep Med Clin* **4**, 165-177 (2009).

19. Everson, C.A., Bergmann, B.M. & Rechtschaffen, A. Sleep deprivation in the rat: III. Total sleep deprivation. *Sleep* **12**, 13-21 (1989).

20. Ferrarelli, F., Smith, R., Dentico, D., Riedner, B.A., Zennig, C., Benca, R.M., Lutz, A., Davidson, R.J. & Tononi, G. Experienced mindfulness meditators exhibit higher parietal-occipital EEG gamma activity during NREM sleep. *PLoS One* **8**, e73417 (2013).

21. Gooley, J.J., Chamberlain, K., Smith, K.A., Khalsa, S.B., Rajaratnam, S.M., Van Reen, E., Zeitzer, J.M., Czeisler, C.A. & Lockley, S.W. Exposure to room light before bedtime suppresses melatonin onset and shortens melatonin duration in humans. *J Clin Endocrinol Metab* **96**, E463-472 (2011).

22. Hafner, M., Stepanek, M., Taylor, J., Troxel, W.M. & van Stolk, C. Why Sleep Matters-The Economic Costs of Insufficient Sleep: A Cross-Country Comparative Analysis. *Rand Health Q* **6**, 11 (2017).

23. Haim, A. & Zubidat, A.E. Artificial light at night: melatonin as a mediator between the environment and epigenome. *Philos Trans R Soc Lond B Biol Sci* **370**(2015).

24. Hakim, F., Wang, Y., Zhang, S.X., Zheng, J., Yolcu, E.S., Carreras, A., Khalyfa, A., Shirwan, H., Almendros, I. & Gozal, D. Fragmented sleep accelerates tumor growth and progression through recruitment of tumor-associated macrophages and TLR4 signaling. *Cancer Res* **74**, 1329-1337 (2014).

25. Hasan, S., Foster, R.G., Vyazovskiy, V.V. & Peirson, S.N. Effects of circadian misalignment on sleep in mice. *Sci Rep* **8**, 15343 (2018).

26. Hastings, M.H., Maywood, E.S. & Brancaccio, M. Generation of circadian rhythms in the suprachiasmatic nucleus. *Nat Rev Neurosci* **19**, 453-469 (2018).

27. Hou, T., Wang, C., Joshi, S., O'Hara, B.F., Gong, M.C. & Guo, Z. Active Time-Restricted Feeding Improved Sleep-Wake Cycle in db/db Mice. *Front Neurosci* **13**, 969 (2019).

28. Kaushal, N., Nair, D., Gozal, D. & Ramesh, V. Socially isolated mice exhibit a blunted homeostatic sleep response to acute sleep deprivation compared to socially paired mice. *Brain Res* **1454**, 65-79 (2012).

29. Kaushal, N., Ramesh, V. & Gozal, D. TNF-alpha and temporal changes in sleep architecture in mice exposed to sleep fragmentation. *PLoS One* **7**, e45610 (2012).

30. Kramer, M. Sleep loss in resident physicians: the cause of medical errors? *Front Neurol* **1**, 128 (2010).

31. Krueger, J.M. The role of cytokines in sleep regulation. *Curr Pharm Des* **14**, 3408-3416 (2008).

32. Krueger, J.M., Rector, D.M. & Churchill, L. Sleep and Cytokines. *Sleep Med Clin* **2**, 161-169 (2007).

33. Landwehr, R., Volpert, A. & Jowaed, A. A Recurrent Increase of Synchronization in the EEG Continues from Waking throughout NREM and REM Sleep. *ISRN Neurosci* **2014**, 756952 (2014).

34. Lazarus, M., Oishi, Y., Bjorness, T.E. & Greene, R.W. Gating and the Need for Sleep: Dissociable Effects of Adenosine A1 and A2A Receptors. *Front Neurosci* **13**, 740 (2019).

35. Lesson 2—Explore Houston, W.H.a.P. *National Institute of Health*.

36. Medicine, I.o. *Sleep Disorders and Sleep Deprivation: An Unmet Public Health Problem*, (The National Academies Press, Washington, DC, 2006).

37. Mesarwi, O., Polak, J., Jun, J. & Polotsky, V.Y. Sleep disorders and the development of insulin resistance and obesity. *Endocrinol Metab Clin North Am* **42**, 617-634 (2013).

38. Mitchell, D.C., Knight, C.A., Hockenberry, J., Teplansky, R. & Hartman, T.J. Beverage caffeine intakes in the U.S. *Food Chem Toxicol* **63**, 136-142 (2014).

39. Nagai, M., Hoshide, S. & Kario, K. Sleep duration as a risk factor for cardiovascular disease- a review of the recent literature. *Curr Cardiol Rev* **6**, 54-61 (2010).

40. Nayak, C.S. & Anilkumar, A.C. Neonatal EEG. in *StatPearls* (Treasure Island (FL), 2020).

41. Nicolaides, N.C., Charmandari, E., Chrousos, G.P. & Kino, T. Circadian endocrine rhythms: the hypothalamic-pituitary-adrenal axis and its actions. *Ann N Y Acad Sci* **1318**, 71-80 (2014).

42. Paul, K.N., Saafir, T.B. & Tosini, G. The role of retinal photoreceptors in the regulation of circadian rhythms. *Rev Endocr Metab Disord* **10**, 271-278 (2009).

43. Peppard, P.E., Young, T., Barnet, J.H., Palta, M., Hagen, E.W. & Hla, K.M. Increased prevalence of sleep-disordered breathing in adults. *Am J Epidemiol* **177**, 1006-1014 (2013).

44. Rasch, B. & Born, J. About sleep's role in memory. *Physiol Rev* **93**, 681-766 (2013).

45. Rezaei, M., Mohammadi, H. & Khazaie, H. EEG/EOG/EMG data from a cross sectional study on psychophysiological insomnia and normal sleep subjects. *Data Brief* **15**, 314-319 (2017).

46. Richardson, G.S., Moore-Ede, M.C., Czeisler, C.A. & Dement, W.C. Circadian rhythms of sleep and wakefulness in mice: analysis using long-term automated recording of sleep. *Am J Physiol* **248**, R320-330 (1985).

47. Roohi-Azizi, M., Azimi, L., Heysieattalab, S. & Aamidfar, M. Changes of the brain's bioelectrical activity in cognition, consciousness, and some mental disorders. *Med J Islam Repub Iran* **31**, 53 (2017).

48. Roth, T. Insomnia: definition, prevalence, etiology, and consequences. *J Clin Sleep Med* **3**, S7-10 (2007).

49. Sims, R.E., Wu, H.H. & Dale, N. Sleep-wake sensitive mechanisms of adenosine release in the basal forebrain of rodents: an in vitro study. *PLoS One* **8**, e53814 (2013).

50. Sleep, Information about Sleep. *National Institute of Health*.

51. Summa, K.C. & Turek, F.W. The Genetics of Sleep: Insight from Rodent Models. *Sleep Med Clin* **6**, 141-154 (2011).

52. Taheri, S., Lin, L., Austin, D., Young, T. & Mignot, E. Short sleep duration is associated with reduced leptin, elevated ghrelin, and increased body mass index. *PLoS Med* **1**, e62 (2004).

53. Valderrama, M., Crepon, B., Botella-Soler, V., Martinerie, J., Hasboun, D., Alvarado-Rojas, C., Baulac, M., Adam, C., Navarro, V. & Le Van Quyen, M. Human gamma oscillations during slow wave sleep. *PLoS One* **7**, e33477 (2012).

54. Veasey, S.C., Valladares, O., Fenik, P., Kapfhamer, D., Sanford, L., Benington, J. & Bucan, M. An automated system for recording and analysis of sleep in mice. *Sleep* **23**, 1025-1040 (2000).

55. Wang, Y., Carreras, A., Lee, S., Hakim, F., Zhang, S.X., Nair, D., Ye, H. & Gozal, D. Chronic sleep fragmentation promotes obesity in young adult mice. *Obesity (Silver Spring)* **22**, 758-762 (2014).

56. Williamson, A.M. & Feyer, A.M. Moderate sleep deprivation produces impairments in cognitive and motor performance equivalent to legally prescribed levels of alcohol intoxication. *Occup Environ Med* **57**, 649-655 (2000).

57. Wurts, S.W. & Edgar, D.M. Circadian and homeostatic control of rapid eye movement (REM) sleep: promotion of REM tendency by the suprachiasmatic nucleus. *J Neurosci* **20**, 4300-4310 (2000).

58. Xie, L., Kang, H., Xu, Q., Chen, M.J., Liao, Y., Thiyagarajan, M., O'Donnell, J., Christensen, D.J., Nicholson, C., Iliff, J.J., Takano, T., Deane, R. & Nedergaard, M. Sleep drives metabolite clearance from the adult brain. *Science* **342**, 373-377 (2013).

59. Yuan, C. & Yang., H. Research on K-Value Selection Method of K-Means Clustering Algorithm. *MDPI* **Volume 2**, 226-235. (2019).

60. Zhang, X., Holt, J.B., Lu, H., Wheaton, A.G., Ford, E.S., Greenlund, K.J. & Croft, J.B. Multilevel regression and poststratification for small-area estimation of population health outcomes: a case study of chronic obstructive pulmonary disease prevalence using the behavioral risk factor surveillance system. *Am J Epidemiol* **179**, 1025-1033 (2014).

# Figures:

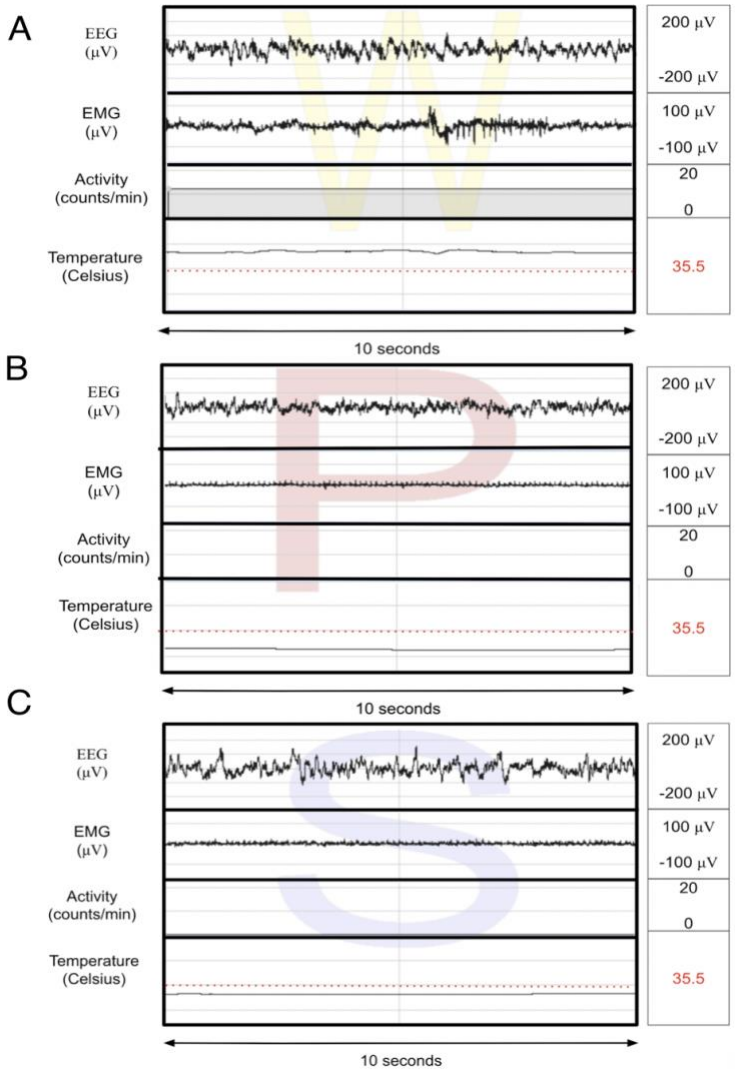


**Figure 1: Examples of manual scoring epochs for REM, NREM, and Wake.**
**(A)** Represents wake epoch with a desynchronized brainwave pattern and high EMG activity. **(B)** Represents REM epoch with a high frequency brainwave pattern and low EMG activity (Muscle Atonia) **(C)** Represents the NREM epoch with high amplitude and low frequency brainwave pattern and low EMG activity.

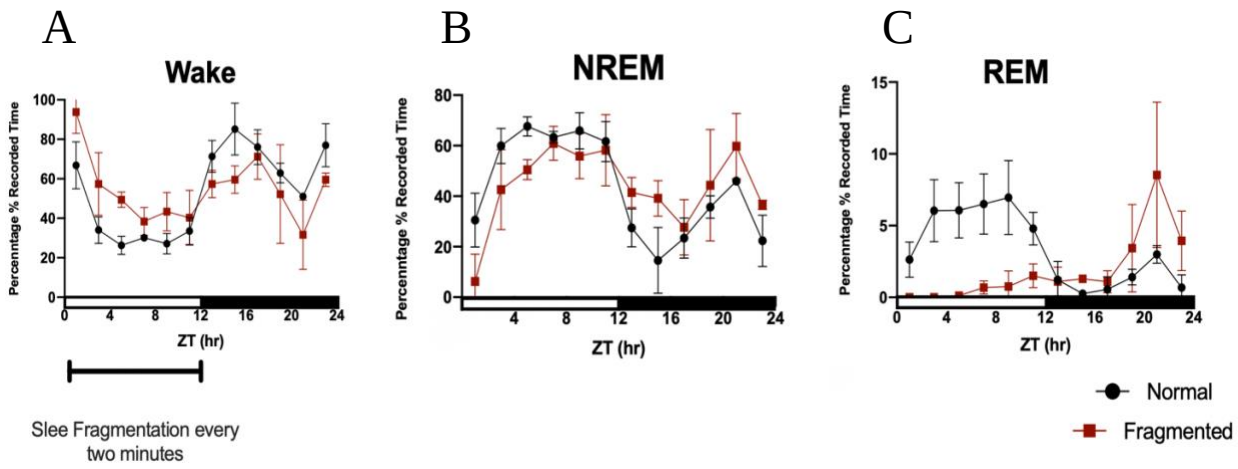


**Figure 2: The Result of manual scoring on normal sleep and first day of sleep fragmentation.** Total of three mice sleep are recorded continuously for 72 hours (72912 epochs), and 24 hours of sleep fragmentation (24296 epochs). **(A)** represents the percentage of recorded time for wake epochs through a 2 hours interval. **(B)** represents the percentage of recorded time for NREM epochs through a 2 hours interval. **(C**) represents the percentage of recorded time for REM epochs through a 2 hours interval.

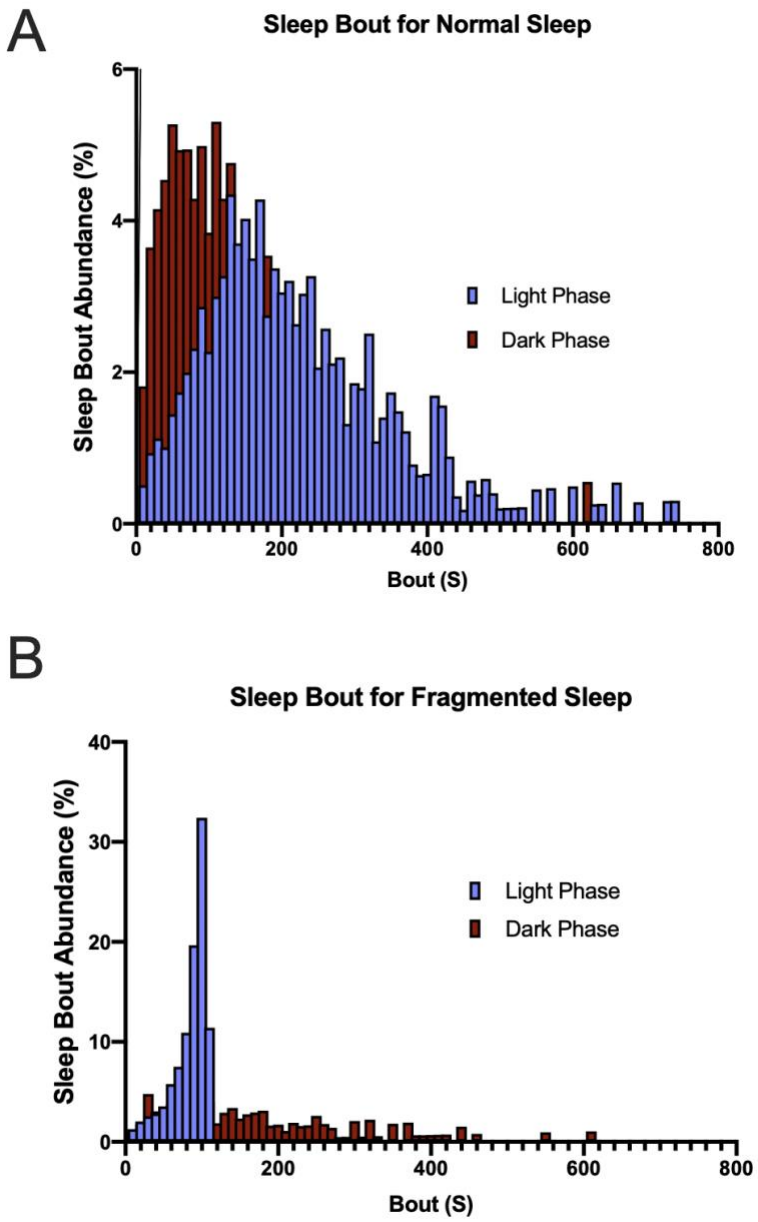


**Figure 3: The distribution of sleep bouts through light phase and dark phase.** The x-axis demonstrates the time from onset of sleep till next wake episode. The Y axis represents the percentage abundance of correspondent sleep bouts during 12 hours of light phase and 12 hours of dark phase for normal sleep **(A)** and fragmented sleep **(B).**

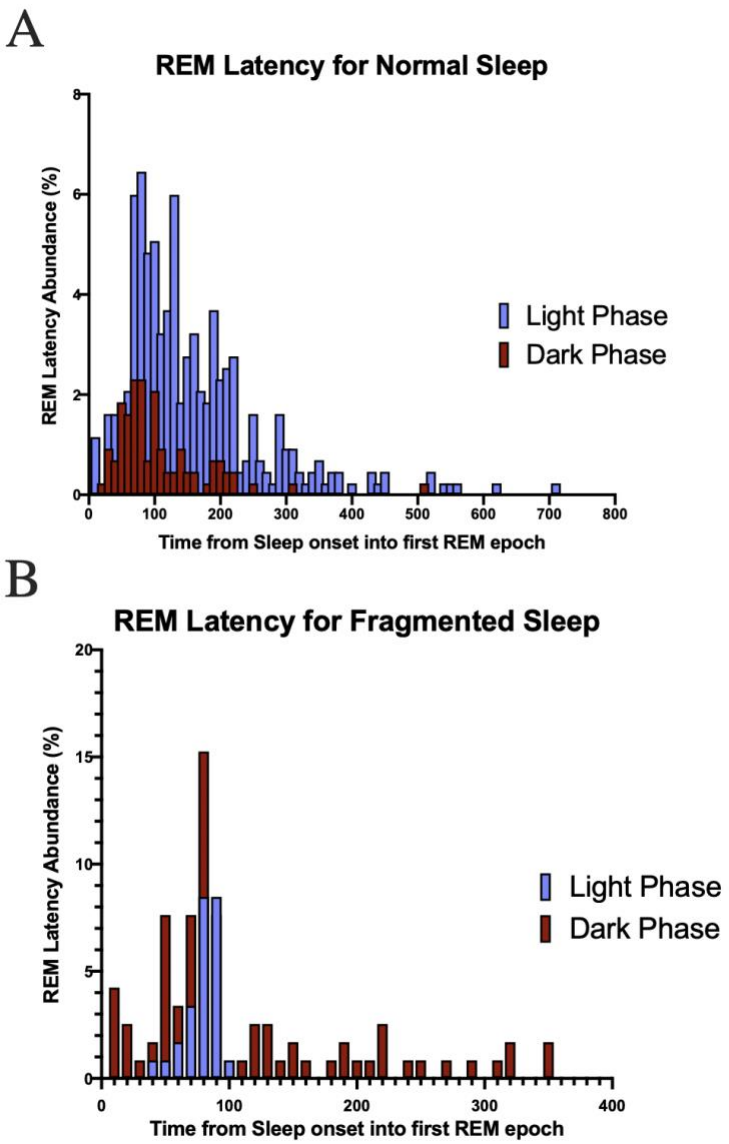


**Figure 4: The distribution of REM Latency through light phase and dark phase.** The x-axis illustrates the time from sleep onset till the first REM episode. The Y axis represents the percentage of the abundance of correspondent x-axis sleep bouts during 24 hours for normal sleep **(A)** and fragmented sleep **(B).**

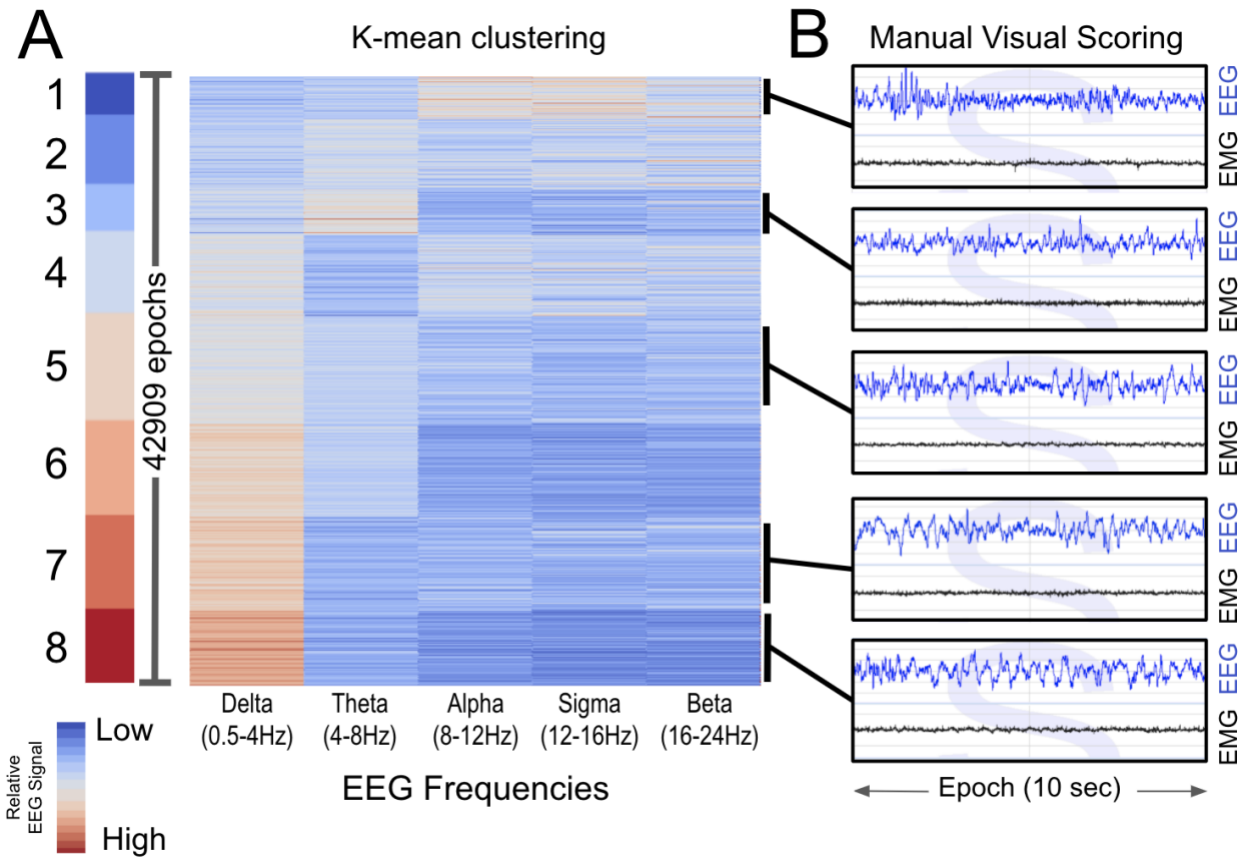


**Figure 5: NREM substages identified by K-mean Clustering and their examples.** (A) represents the result of K-Mean Clustering based on the five brain wave patterns that have distinct frequencies. The cluster number is assigned based on their delta ratios in increasing order. (B) shows the five manually scored epochs of NREM sleep that have distinctive amplitudes and frequencies.

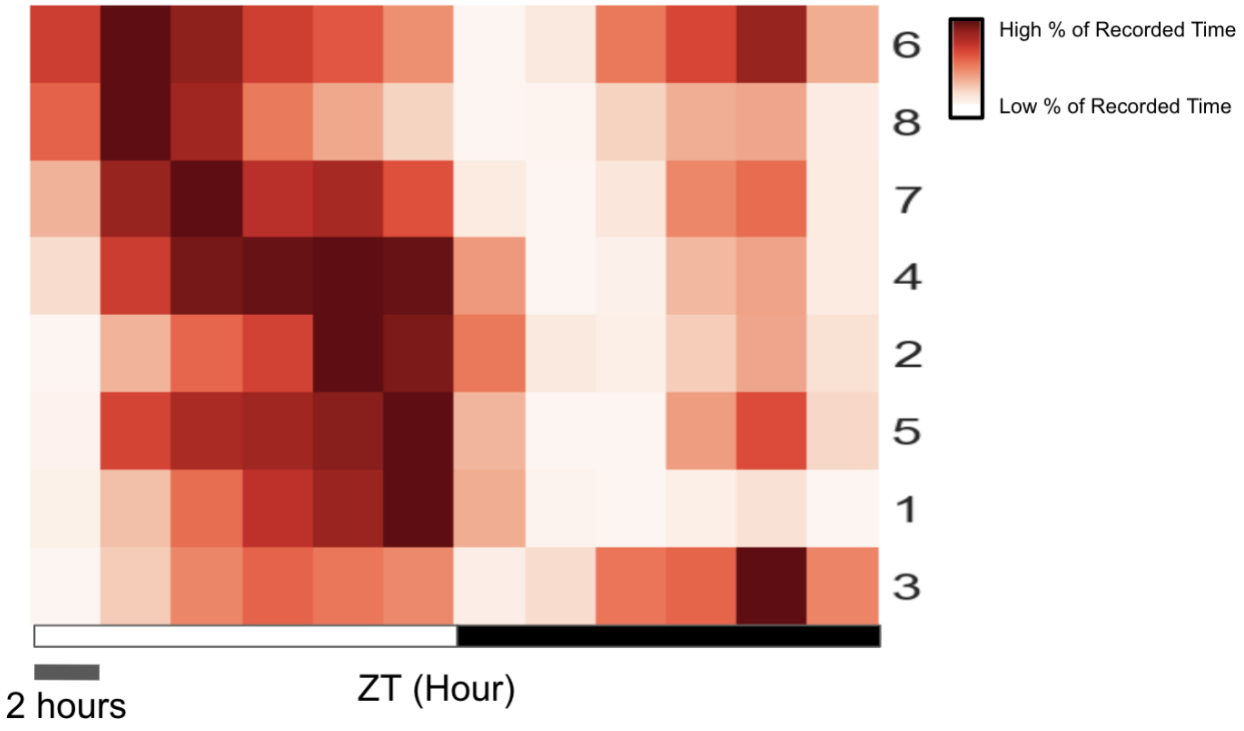


**Figure 6: Temporal pattern of normal NREM sleep clusters in respect to their temporal peaks.** Each square represents a two hours interval through 24 hours. The clusters are ordered based on the early appearance of their temporal peaks.

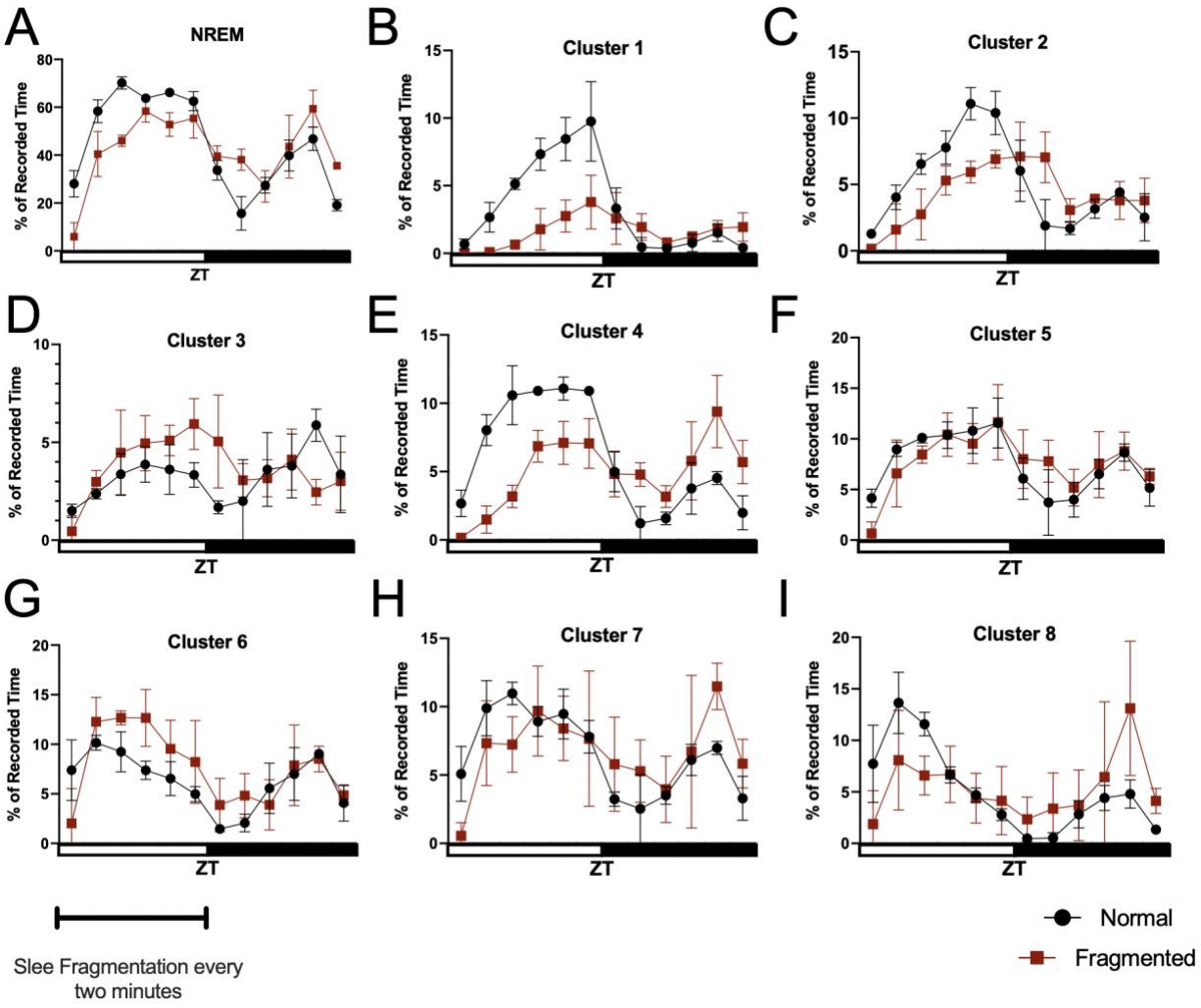


**Figure 7: Result of acute sleep disruption impact on the temporal distribution of NREM substages. (A)** represents the temporal pattern of NREM sleep. **(H)** and **(I)** demonstrate clusters 7 and 8 respectively as their peaks shift into the dark phase. **(F)** represents cluster 5 is impacted the least by fragmentation. **(D)** and **(G)** represent clusters 3 and 6 which have higher percentages in fragmentation. **(B)**, **(C)**, and **(E)** represent clusters 1, 2, and 4 which have decreased percentages during fragmentation.

Raw Data Distribution Z-Scored Data Distribution

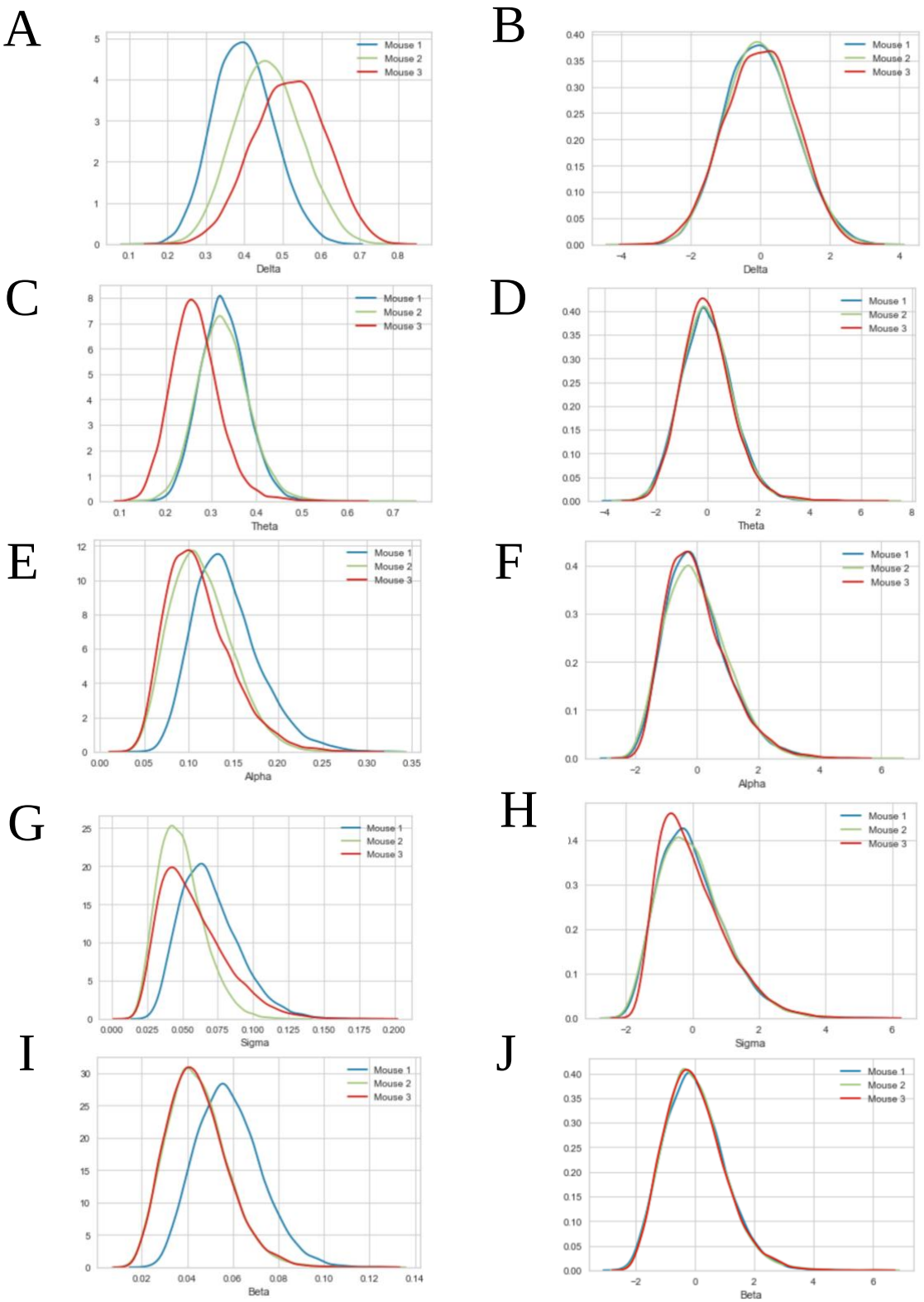


**Figure 8: The brainwave data distribution before and after normalization. (A, C, E, G, I)** represent the distribution of delta, theta, alpha, sigma and beta power ratios respectively for three mice. **(B, D, F, H, J)** represent the data after normalization by z-score.

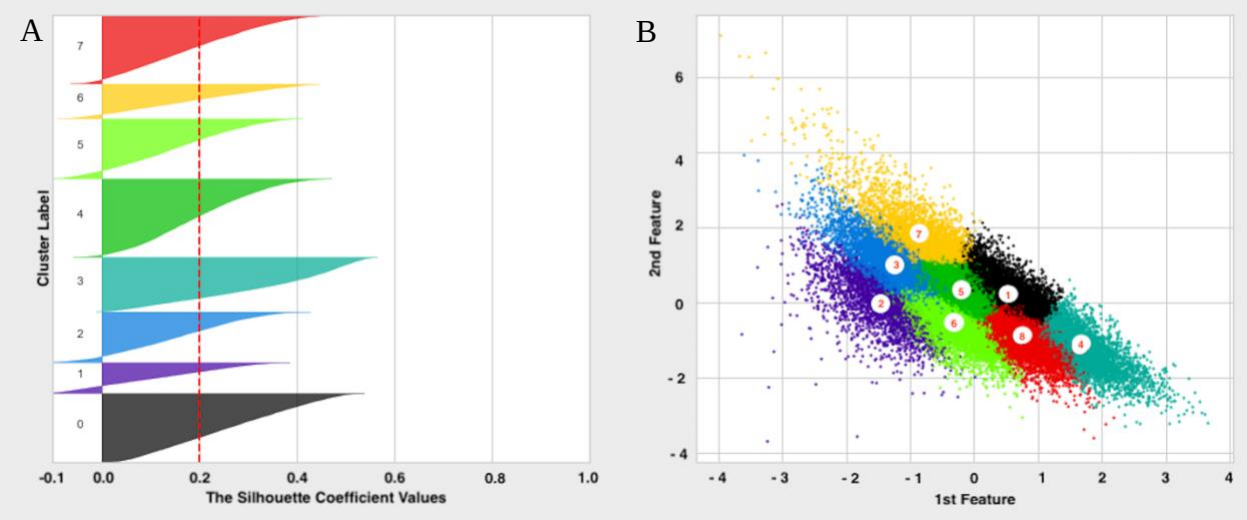


**Figure 9: Silhouette Analysis for K-Mean clustering on sample data with 8 number of clusters. (A)** represents the silhouette plot for various clusters. **(B)** represents the visualization of the clustered data for total of 42909 epochs of NREM.

# Tables:

### Conventional Sleep Parameters

**Table 1:** demonstrates the duration of mice sleep, NREM percentage, REM percentage, and sleep bouts for three mice in 72 hours of normal sleep and first day of sleep fragmentation in 24 hours (T), 12 hours light phase (L), and 12 hours dark phase (D).

| | **Normal** | **Fragmented** |
|---|---|---|
| **Time Spent Asleep in 24 Hours (Min)** | T: 644.09 ± 10.40<br>L:448.24 ± 8.86<br>D: 195.85 ± 18.39 | T:617.94 ± 115.00<br>L: 304.61 ± 68.05<br>D: 313.33 ± 51.88 |
| **Percentage of Time Spent in NREMS** | T: 44.25 ± 2.14<br>L: 58.22 ± 1.56<br>D: 29.06 ± 3.18 | T: 43.71 ± 7.43<br>L: 45.90 ± 9.53<br>D: 41.67 ± 5.90 |
| **Percentage of Time Spent in REMS** | T: 3.45 ± 1.07<br>L: 5.50 ± 1.75<br>D: 1.22 ± 0.46 | T: 1.95 ± 0.37<br>L: 0.52 ± 0.38<br>D: 3.29 ± 1.02 |
| **Sleep Bout (seconds)** | T: 107.04 ± 0.81<br>L: 137.67 ± 1.67<br>D: 75.20 ± 1.31 | T: 77.60 ± 2.12<br>L:69.26 ± 6.57<br>D: 87.63 ± 1.57 |

## NREM Cluster Percentage

**Table 2:** demonstrates the percentage recorded time of clusters for three mice in 72 hours of normal sleep and first day of sleep fragmentation in 24 hours (T), 12 hours light phase (L), and 12 hours dark phase (D).

| | Normal | Fragmented |
|---|---|---|
| **Cluster 1** | T: 3.72 ± 0.99<br>L: 4.87 ± 0.57<br>D: 2.51 ± 1.53 | T: 1.73 ± 0.70<br>L: 1.59 ± 0.68<br>D: 1.86 ± 0.73 |
| **Cluster 2** | T: 5.20 ± 0.46<br>L: 5.96 ± 0.45<br>D: 4.41 ± 1.40 | T: 4.55 ± 0.19<br>L: 4.10 ± 0.82<br>D: 4.97 ± 0.95 |
| **Cluster 3** | T: 3.18 ± 0.22<br>L: 2.87 ± 0.69<br>D: 3.50 ± 0.27 | T: 3.84 ± 0.42<br>L: 4.18 ± 0.69<br>D: 3.52 ± 0.69 |
| **Cluster 4** | T: 6.29 ± 0.29<br>L: 8.24 ± 0.85<br>D: 4.27 ± 0.56 | T: 5.30 ± 0.76<br>L: 4.66 ± 0.90<br>D: 5.90 ± 0.70 |
| **Cluster 5** | T: 7.72 ± 0.55<br>L: 8.71 ± 0.41<br>D: 6.70 ± 0.88 | T: 7.94 ± 1.81<br>L: 8.50 ± 2.11<br>D: 7.41 ± 1.64 |
| **Cluster 6** | T: 6.45 ± 0.46.<br>L: 7.63 ± 0.87<br>D: 5.21 ± 0.70 | T: 7.82 ± 2.32<br>L: 10.01 ± 2.61<br>D: 5.77 ± 2.09 |
| **Cluster 7** | T: 6.74 ± 0.42<br>L: 8.30 ± 0.36<br>D: 5.12 ± 0.67 | T: 6.96 ± 2.10<br>L: 7.29 ± 2.51<br>D: 6.65 ± 1.72 |
| **Cluster 8** | T: 5.37 ± 0.45<br>L: 8.00 ± 0.38<br>D: 2.64 ± 0.69 | T: 5.58 ± 2.84<br>L: 5.57 ± 2.93<br>D: 5.59 ± 2.22 |

## Distribution of NREM Substages from Three Mice

**Table 3:** illustrates the percentage of NREM sleep associated with each NREM clusters for three mice during 72 hours of normal sleep recording and one day of sleep fragmentation.

| Cluster Number | Mouse 1 | Mouse 2 | Mouse 3 |
|---|---|---|---|
| **1** | 29.84% | 34.29% | 35.87% |
| **2** | 31.69% | 34.68% | 33.63% |
| **3** | 37.01% | 32.87% | 30.12% |
| **4** | 36.91% | 34.12% | 28.97% |
| **5** | 33.87% | 31.59% | 34.54% |
| **6** | 34.58% | 33.38% | 32.04% |
| **7** | 32.30% | 32.32% | 35.19% |
| **8** | 29.23% | 34.68% | 36.10% |

This thesis is coauthored with Dr. Michael Lam and Fred Monroe. The thesis author was the primary author of this paper.